



# Co-administration of L-Ascorbic Acid and $\alpha$ -Tocopherol Alleviates Arsenic-Induced Immunotoxicities in the Thymus and Spleen by Dwindling Oxidative Stress-Induced Inflammation

Jeet Maity<sup>1</sup> · Priyankar Pal<sup>1</sup> · Ranjana Pal<sup>1</sup> · Prabir Kumar Mukhopadhyay<sup>1</sup>

Received: 20 June 2023 / Accepted: 1 September 2023 / Published online: 13 September 2023  
© The Author(s), under exclusive licence to Springer Science+Business Media, LLC, part of Springer Nature 2023

## Abstract

Herein, we investigated whether L-ascorbic acid (L-AA) and  $\alpha$ -tocopherol ( $\alpha$ -T) co-administration has the potential to alleviate arsenic-induced immunotoxicities in the thymus, spleen, and circulating leukocytes. Forty-eight adult male Wistar rats were randomly divided into four groups before the treatment: group I (control); group II (sodium arsenite, 3 mg/kg/day/rat); group III (sodium arsenite + L-AA (200 mg/kg/day/rat) and  $\alpha$ -T (400 mg/kg/day/rat)); group IV (L-AA and  $\alpha$ -T). The result showed that sodium arsenite exposure (consecutive 30 days) caused weight reduction, structural alterations in the thymus and spleen, accompanied by a decrease in thymocyte and splenocyte count. Decreased superoxide dismutase and catalase activity, increased malondialdehyde and protein–carbonyl content, reduced Nrf2 and Bcl2 expression, and increased p-ERK, NF- $\kappa$ B, Bax, and cleaved-caspase-3 expression were also observed in the thymus and spleen of arsenic-exposed rats. Enhanced plasma ACTH and corticosterone, ROS-induced apoptosis of lymphocytes were also observed. L-AA and  $\alpha$ -T co-administration has the potential to abrogate the deleterious impact of arsenic on the thymus, spleen, and circulating lymphocytes. Whole transcriptome analysis of leukocytes revealed that arsenic treatment augmented the expression of Itga4, Itgam, and MMP9 genes, which might help in transient migration of the leukocytes through the endothelial cell layer. Co-administration with L-AA and  $\alpha$ -T maintained Itga4, Itgam, and MMP9 gene expression within leukocytes at a lower level.

**Keywords** Immunotoxicity · Arsenic · Thymus · Spleen · Leukocyte transcriptome · L-Ascorbic acid and  $\alpha$ -tocopherol

## Introduction

According to the Agency for Toxic Substances and Disease Registry (ATSDR), arsenic contamination is a global human health concern [1]. It is the twentieth most plentiful element on the planet, which can be found as a sulphide (realgar [As<sub>4</sub>S<sub>4</sub>]; orpiment [As<sub>2</sub>S<sub>3</sub>]), oxide (arsenic trioxide [As<sub>2</sub>O<sub>3</sub>]; sodium meta arsenite [NaAsO<sub>2</sub>]; sodium arsenate [Na<sub>3</sub>AsO<sub>4</sub>]), or metal salt (arsenopyrite [FeAsS] and enargite [Cu<sub>3</sub>AsS<sub>4</sub>]) [2]. It is a group V element that has a plethora of electron and empty orbitals that stabilises the oxidation number from –3 to +5. The configuration of electron of neutral arsenic is [As] 3d<sup>10</sup> 4s<sup>2</sup> 4p<sub>x</sub><sup>1</sup> 4p<sub>y</sub><sup>1</sup> 4p<sub>z</sub><sup>1</sup> — a state that provides up to 5 valence electrons for involvement in atomic

bonding and P orbitals that are not filled allow for electron occupancy. Arsenic forms an oxo-anion arsenite (H<sub>3</sub>As<sup>3+</sup>O<sub>3</sub>) and arsenate (H<sub>3</sub>As<sup>5+</sup>O<sub>4</sub>) in aqueous solution.

The metabolic products of arsenic play an important role in the development of toxicity within physiological system. This metabolism includes the transformation of inorganic arsenic into monomethylarsonous acid, dimethylarsonous acid, monomethylarsonic acid, and dimethylarsonic acid. Trivalent arsenicals are more toxic than pentavalent arsenicals due to increased cellular uptake and accumulation [3], lower excretion rate, and a higher affinity for thiols and sulfhydryl groups of proteins in various organs [4]. More than 200 enzymes are known to be inhibited by these trivalent forms [3].

Ingesting food or drinking of water contaminated with arsenic is the main way through which people get arsenic into their systems. According to the World Health Organization (WHO), the recommended range for arsenic in drinking water is 10  $\mu$ g/l. It was shown in China that the average amount of arsenic consumed from ingested rice is 2  $\mu$ g/kg

✉ Prabir Kumar Mukhopadhyay  
prabir.dbs@presiuniv.ac.in

<sup>1</sup> Department of Life Sciences, Presidency University, 86/1 College Street, Kolkata 700073, India

of body weight [5]. The overall scenario regarding drinking water adulteration by arsenic is most dreadful in South-East Asia including India, China, Vietnam, Philippines, and Bangladesh [6]. In Baghdad and Iraq, arsenic level was found to be substantially higher (36 mg/kg) in soil [7]. An old mining site in Zlatna area of Romania was discovered to have increased soil levels of arsenic [8]. A study conducted in Hungary and Pannonian basin indicated that the groundwater and soil had a noticeably greater content of arsenic [9]. In India, the principal sources of arsenic are delta sediments and Gangetic River basin in Shilling Plateau and Himalayan Mountain. The Bihar mica belt and Gondaranya coal belt in the Raajmahal basin in eastern India, Vindhya range in central India, are other geological sources of arsenic [10].

Over 500 million individuals worldwide are exposed to arsenic-contaminated water at a level higher than the permissible level suggested by the WHO (10 µg/l) [11]. Arsenic toxicity manifests itself in a variety of ways in the human body including hyperkeratosis and hyperpigmentation in the integumentary system, dark warts on the skin, and weakened central and peripheral nervous system [12–14]. A research conducted in Hungary, Romania, and Slovakia showed a direct link between the arsenic content in groundwater and the prevalence of basal cell carcinoma [15]. Recently, it has been reported that arsenic contamination in the Indo-Gangetic plains of Bihar leads to an increase in cancer risk [16].

Chronic arsenic exposure leads to immune suppression which in turn leads to increased risk of opportunistic infections and diseases like tuberculosis and hepatitis E [17, 18]. Likewise, in utero exposure to arsenic impairs an infant's thymic development with increased morbidity due to possible immune suppression [19–21]. In 2017, Duan et al. reported that arsenic causes decrease in size and weight of both the thymus and spleen of arsenic-exposed C57BL/6 mice [1]. Moreover, acute arsenic exposure led to activation of MAPK/NF-κβ signalling pathway which was linked with the inflammation in the thymus and spleen of female C57BL/6 mice by enhancing the secretion of pro-inflammatory cytokines [1]. In 2016, Xu et al. showed that there was a positive correlation in between intracellular monomethylarsonous (MMA<sup>3+</sup>) acid and DNA damage in thymic cells [22]. This MMA<sup>3+</sup> which is much more toxic than As<sup>3+</sup> is generated from As<sup>3+</sup> within the liver in the presence of arsenic-3-methyltransferase [22]. Another study showed that mitochondrial degeneration and aberrant nucleus with heterochromatinisation were evident in thymic lymphocytes of mice exposed to 5 ppm, 15 ppm, and 300 ppm arsenic [23]. In the same study, there was also a significant dose-dependent increase in intercellular gap as well as irregular branched cytoplasmic projection and aberrant nuclei in arsenic-exposed splenic cells [23]. Sub-chronic arsenic exposure caused hyalinosis and sclerosis of small blood vessels

and interstitial tissue hyperplasia of spleen [24]. Apart from these, arsenic exposure suppressed mitogen-induced T cell proliferation and cytokine secretion [25, 26]. On the other hand, long-term arsenic exposure leads to time-dependent modulation of inflammation and immunosuppression in the spleen [27]. In earlier studies, it has been shown that arsenic caused increase in the secretion of ACTH and subsequently elevated the plasma corticosterone level [28, 29]. It is well known that elevated plasma corticosterone level leads to apoptosis of CD4<sup>-</sup>/CD8<sup>-</sup> T cells, CD4<sup>+</sup>/CD8<sup>+</sup> double-positive T cells, CD4<sup>+</sup>/CD8<sup>-</sup> T cells, and CD8<sup>+</sup>/CD4<sup>-</sup> T cells and results in thymic involution [30, 31]. Elevated plasma corticosterone level also causes involution of spleen [32]. Until now, there is no data available regarding arsenic-mediated elevated plasma corticosterone-induced apoptosis of thymocytes and splenocytes.

To the best of our knowledge, there is no safe therapy available for arsenic-induced immunotoxicities which are unremitting mare's nest in the present day. Moreover, certain important chelating drugs, such as meso-2,3-dimercaptosuccinic acid, sodium 2,3-dimercaptopropane-1-sulfonate, monoisoamyl-meso-2,3-dimercaptosuccinic-acid, and monocyclohexyl-meso-2,3-dimercaptosuccinic-acid, have serious repugnant effects by interfering with usual cellular metabolism [33, 34]. Natural antioxidants are therefore thought to be the most effective agents in decreasing the oxidative stress caused by arsenic. Nowadays, nutraceuticals have drawn the attention of researchers, since some nutraceuticals have anti-oxidant properties and ability to modulate epigenome, which can be used to combat heavy metal toxicities. Among such nutraceuticals, ascorbic acid and α-tocopherol are popular for their anti-oxidant and anti-inflammatory activities. To date, the combined impact of L-ascorbic acid (L-AA) and α-tocopherol (α-T) on arsenic-induced apoptosis in the thymus and spleen has not been studied.

Based on the abovementioned insights, this study was designed to investigate the possible ameliorative potential of L-AA and α-T in reducing arsenic-induced immunotoxicities such as structural and functional anomalies in the thymus, spleen, and circulating immune cells.

## Materials and Methods

### Chemicals

Sodium (meta) arsenite (Aldrich, Cat. No. S7400-100G); L-ascorbic acid, extra pure (SRL, Code: 0149100); ± α-tocopherol (HiMedia, Code: CMS185-50G); Haematoxylin stain (HiMedia, Code: TC259-100G); Eosin-Y (MERCK, Cas No. 17372-87-1); Immobilon-P26.5X3.75 M roll PVDF 0.45 UM (Millipore, Item No.

IPVH00010); Primary antibody against Nrf2 (GeneTex, Cat. No. GTX135165), Bcl2 (Bio-Bharti Life Science Pvt. Ltd, Cat. No. BB-AB0230), Bax (Bio-Bharti Life Science Pvt. Ltd, Cat. No. BB-AB0250),  $\beta$ -actin (Bio-Bharti Life Science Pvt. Ltd, Cat. No. BB-AB0024), Caspase-3 (Cell Signaling Technology, Cat. No. 8G10), Cleaved-Caspase-3 (Asp175) (Cell Signaling Technology, Cat. No. 5A1E); NF- $\kappa$ B p65 (Gene Tex, Cat No. GTX102090); ERK1/2 (Gene Tex, Cat No. GTX635617); p-ERK (Gene Tex, Cat No. GTX129275); Goat anti-rabbit IgG (H + L), alkaline phosphatase (AP)-conjugated secondary antibody (Invitrogen™, REF-A16107), Alexa Fluor™ 488 goat anti-rabbit IgG (H + L) secondary antibody (Invitrogen™, REF-A11008); BCIP/NBT colour development substrate (PROMEGA, REF-S3771); Histopaque-1077 (SIGMA, Code: 10771-100ML); Agarose special, low EEO (HiMedia, Cat. No. MB002-10G); Agarose (BIORON, Cat. No. 604001); H2DCFDA (Invitrogen™, REF-D399); Dead cell apoptosis kit with FITC-annexin-V/PI for flow cytometry (Invitrogen™, Cat. No. V13242).

## Experimental Animals

Forty-eight adult male Wistar rats (weighing  $125 \pm 5$  g; 6–7 weeks old) were purchased from the registered animal breeding house (M/s Chakraborty Enterprise; CPCSEA Regd. No. 1443/PO/b/11/CPCSEA) and rats were maintained in polypropylene cage (4 rats per cage) in controlled condition (room temperature  $25 \pm 2$  °C, normal photoperiod of 12-h light/dark environment). The animals were given standard laboratory food diet (71% carbohydrate, 7% fat, 18% protein [6.32% wheat flour, 4.38% barley meal, and 10% casein], and 4% salt mixture) [35] and sufficient amount of water. The animals were allowed to acclimatise to the laboratory conditions for 7 days before the commencement of experiment. All animal experiments were carried out as per animal ethical guidelines given by institution animal ethical committee of Presidency University (Sanction No. PU/IAEC/PM/24).

## Experimental Design

Adult male Wistar rats were randomly divided into four (4) groups. The groups were as follows: group I (control group); group II (sodium arsenite-treated group) received sodium arsenite at 3 mg/kg BW (body weight)/day dose through oral gavage; group III (sodium arsenite + L-AA +  $\alpha$ -T group) received sodium arsenite, L-AA, and  $\alpha$ -T through oral gavage at 3 mg/kg BW/day, 200 mg/kg BW/day, and 400 mg/kg BW/day dose respectively; group IV (only L-AA +  $\alpha$ -T group) received L-AA and  $\alpha$ -T through oral gavage at 200 mg/kg BW/day and 400 mg/kg BW/day dose respectively. Sodium arsenite stock solution was prepared from

which group II and group III were gavaged with 3 mg/kg BW/day for 30 consecutive days [36, 37]. The LD50 of arsenic in rat was documented as 40 mg/kg BW/day and the dose of sodium arsenite (3 mg/kg BW/day) was chosen based on the OECD (Organization of Economic Corporation) criteria for testing of chemicals and previous dose-dependent arsenic toxicity studies on rodent [24, 33, 38, 39]. Arsenic dosage has been chosen at 3 mg/kg BW, which is 1/13th of its LD50 dose. L-AA and  $\alpha$ -T were dissolved in distilled water and olive oil (Bertoli extra virgin olive oil), respectively. All the treatments were continued for 30 consecutive days. At the end of the treatment period, the animals were euthanised after overnight fasting. The whole thymus, spleen, and blood were collected and subjected to subsequent experiments (Fig. 1).

## Tissue and Blood Collection

The thymus and spleen were promptly removed from sacrificed animal and washed in 0.9% normal saline and small slices of both tissues were subjected to histological studies and the remaining portion of tissues were harvested for all subsequent experiments.

The blood was collected from anaesthetised animals under sterile condition by cardiac puncture using 18-gauge needle attached with glass syringe and kept in both heparinised and EDTA (ethylenediaminetetraacetic acid) vial for biochemical and haematological analysis, respectively.

## Calculation of Thymus and Splenic Index

According to the following formula, the thymus and splenic indexes were determined [1]:

$$\text{Thymus index} = \left[ \frac{\text{Thymus weight}}{\text{Body weight}} \right] \times 100\%$$

$$\text{Spleen index} = \left[ \frac{\text{Spleen weight}}{\text{Body weight}} \right] \times 100\%$$

## Histology of the Thymus and Spleen

After removal of thymus and spleen from the sacrificed animal, the organs were fixed in neutral buffered formalin solution (composed of formaldehyde, sodium phosphate monobasic [ $\text{NaH}_2\text{PO}_4$ ], and sodium phosphate dibasic [ $\text{Na}_2\text{HPO}_4$ ]) and processed for paraffin-embedding. Thin paraffin Sects. (5  $\mu\text{M}$ ) were obtained using rotary microtome (Leica microtome). Then thin sections were stained by routine haematoxylin–eosin stain for photo-microscopy (Zeiss, Thornwood, NY, USA) analysis of histopathology of the above-mentioned tissues [35].

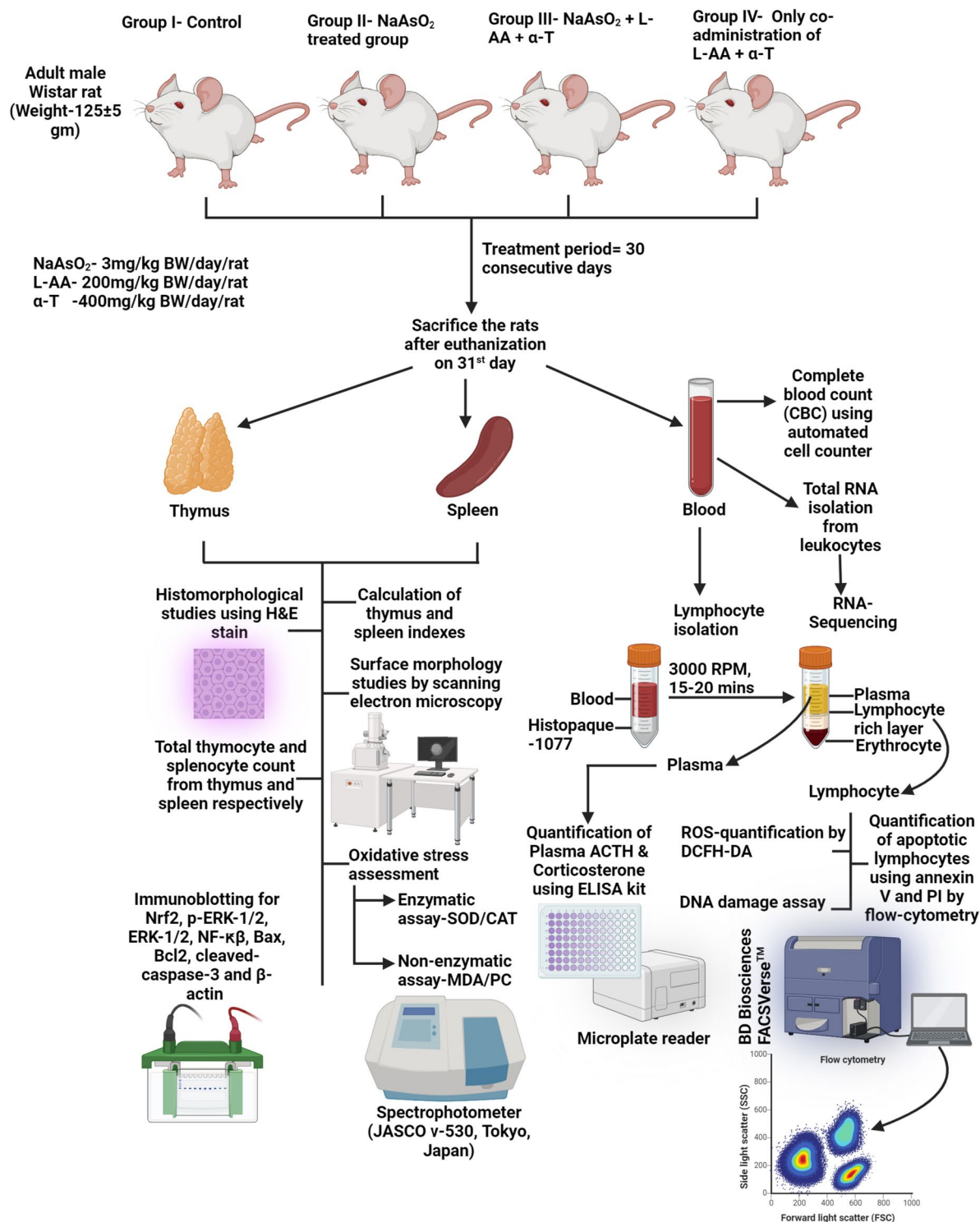


**Fig. 1** Experimental design — adult male Wistar rats were randomly divided into four groups. Group I — control group; group II was received sodium arsenite (NaAsO<sub>2</sub>) at 3 mg/kg/BW/day. Group III was supplemented with L-AA and α-T at 200 mg/kg/BW/day and 400 mg/kg/BW/day respectively after treatment with sodium arsenite at aforesaid dose level. At cull, thymus and spleen and blood were aseptically collected. The thymus and spleen were analysed for alteration of histoarchitecture and surface morphology, SOD (superox-

ide dismutase), CAT (catalase) activity, MDA (malondialdehyde) and PCC (protein carbonyl content), Nrf2 (nuclear factor erythroid 2-related factor 2) expression, and intrinsic apoptosis pathway assessment. Isolation of lymphocytes from whole blood and analysed for quantification of ROS (reactive oxygen species) generation using DCFH-DA, quantification of apoptotic cells using annexin-V/PI staining, and DNA damage assay (created with BioRender.com)

## Scanning Electron Microscopy

Dissected thymus and spleen were diced into tiny pieces and fixed for 48 h at room temperature using 2.5% glutaraldehyde in 0.2 M phosphate buffer. Fixed tissues were then dehydrated using ethanol in increasing concentration (50–100%), immersed in chilled acetone, and allowed to air dry for an entire day. The dried tissues were fixed on aluminium stubs. Following a platinum coating, coated tissues were studied via scanning electron microscope (Zeiss EVO-18 special edition, Germany) [33].

## Measurement of the Plasma ACTH Level

A commercially available ELISA kit for ACTH (analytical sensitivity 6 pg/ml, range — 7.81–500 pg/ml, Mouse/Rat ACTH ELISA kit (abcam) Cat No. ab263880) was used to analyse plasma samples.

## Measurement of the Plasma Corticosterone

A commercially available ELISA kit for corticosterone (range — 15–2250 ng/ml, analytical sensitivity 6.1 ng/ml, Rat corticosterone ELISA kit (Crystal Chem High Performance Assays) Cat No. 80554) was used to analyse plasma samples.

## Thymic Lymphocyte Isolation

Through mechanical disruption between frosted glass slides, lymphocytes were released from thymic lobes. After that, the cells were washed with 1X phosphate buffer solution. Following centrifugation for 5 min at 4 °C at 1500 rpm, the cell pellets were washed thrice with 1X phosphate buffer solution and filtered through 70- $\mu$ m cell strainer and enumerated by using haemocytometer [40].

## Splenic Lymphocyte Isolation

The spleen was removed from the sacrificed rat and instantly immersed in Alsever's solution (composed of sodium citrate (dihydrate) 8.0 g/L, citric acid (monohydrate) 0.55 g/L, glucose 20.5 g/L, sodium chloride 4.2 g/L). Splenic cells were liberated by mechanical dissociation using frosted glass slides. Until a single cell suspension was attained, cells were repeatedly aspirated using sterile Pasteur pipette. After that, single cell suspension was transferred into sterile tubes and kept on ice to allow the cell debris to settle down. After that, supernatant was layered onto 3 ml of Histopaque-1077 and centrifuged for 15 min at 3000 rpm. Then the opaque interface, lymphocyte rich layer, was carefully aspirated by sterile Pasteur pipette and washed with 1  $\times$  PBS. After that, it was enumerated by using a haemocytometer [41].

## Assessment of Oxidative Stress Within the Thymus and Spleen

### Enzymatic Parameters

**Superoxide Dismutase (SOD)** Tissue homogenisation was performed in chilled 0.1 M phosphate buffer (pH 7.2) at 25 mg/ml. The homogenates were centrifuged for 10 min at 10,000 g in 4 °C. The enzyme activity was assessed by quantifying the spontaneous auto-oxidation of haematoxylin after adding and without adding the supernatant of homogenised tissue to a medium having 0.1 M phosphate buffer and 0.5 mM EDTA [33, 42]. Finally, the enzymatic activity was determined by spectrophotometer (JASCO v-530, Tokyo, Japan) at 560 nm and activity will be expressed in unit/mg tissue [33, 35].

**Catalase (CAT)** Homogenisation of tissues in each group was done in chilled 0.05 M Tris-HCL buffer (pH 7.0) at a tissue concentration of 20 mg/ml [33, 35]. Then the tissue homogenates were centrifuged at 10,000 g in 4 °C for 20 min. The catalase activity was determined based on the biochemical method described by Claiborne [43]. Spectrophotometric analysis of decomposition of hydrogen peroxide ( $H_2O_2$ ) to water ( $H_2O$ ) and  $O_2$  by catalase present in supernatant at 240 nM was expressed in  $\mu$ M  $H_2O_2$  consumed/mg tissue/min [33, 35].

### Non-enzymatic Parameters

**Malondialdehyde (MDA) Production** This biochemical test is based on the theory that MDA is produced as a by-product of omega-3 and omega-6 fatty acid peroxidation, which interacts with thiobarbituric acid to generate a luminous red adduct [33, 35]. Thymic and splenic tissue samples were homogenised in 0.1 M phosphate buffer with a pH of 7.4 at 25 mg/ml, followed by centrifugation for 5 min at 15,000  $\times$  g at 4 °C. The supernatant (0.5 ml) was collected and mixed with 0.5 ml of 0.95% saline and 2 ml of a 2-thiobarbituric acid-trichloroacetic acid (TBA-TCA) combination and heated for 10 min [33, 35]. Before centrifugation, the entire mixture was permitted to chill at room temperature. The mixture was then centrifuged for 10 min at 3200 g [33, 35]. The whole supernatant was placed in a spectrophotometric cuvette, and the absorbance at 535 nm (JASCO v-530, Tokyo, Japan) was measured, and the concentration of MDA was determined in nM per mg tissue [33, 35].

**Protein-Carbonyl Content** Following treatment with 2–4-dinitrophenylhydrazine (2–4-DNPH), the carbonyl content of thymic and splenic protein was measured [33, 35]. The carbonyl group of oxidised protein may be measured

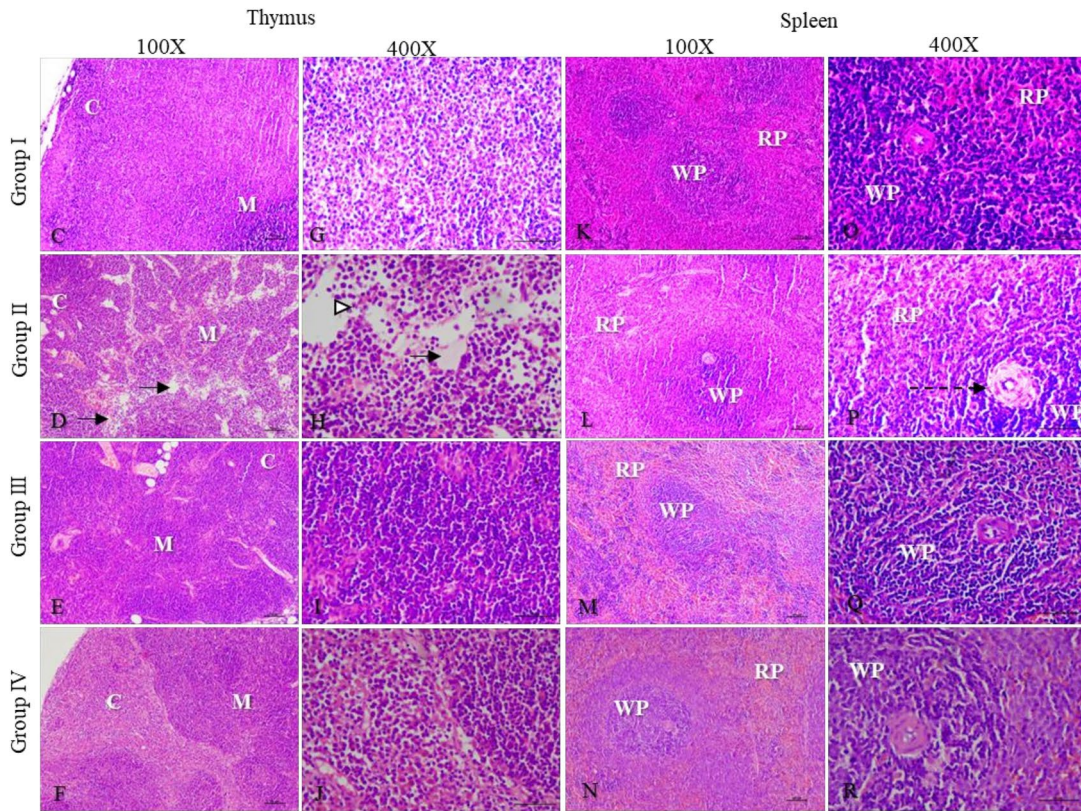
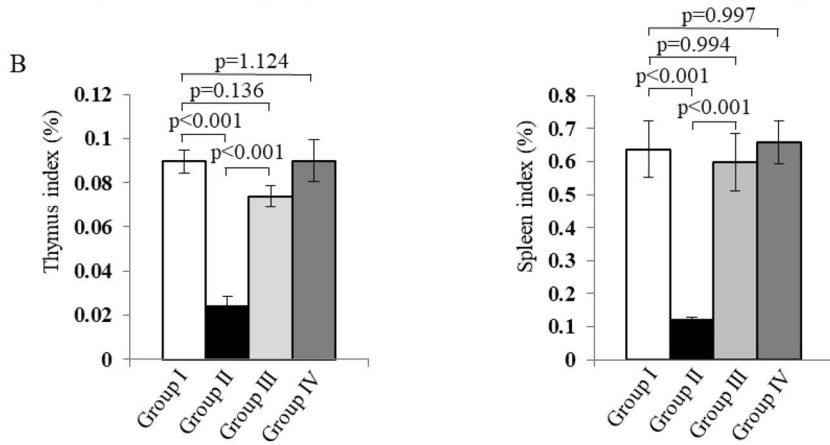
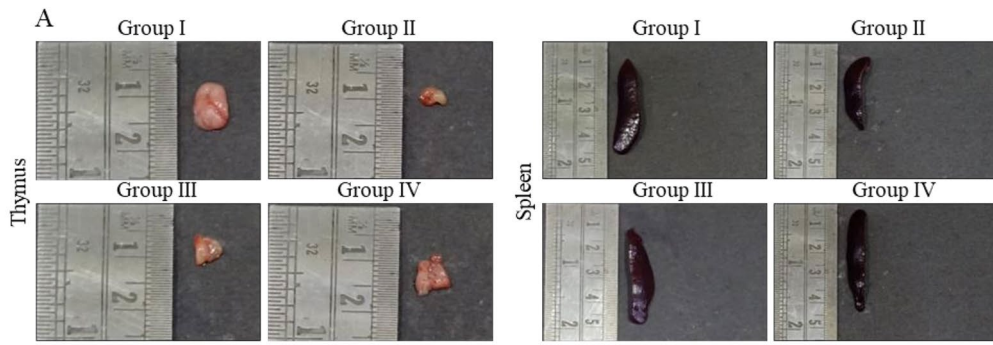


**Fig. 2** Ameliorative effect of supplementation with L-AA and  $\alpha$ -T on arsenic-induced alterations of tissue size and histoarchitecture of the thymus and spleen ( $n=3$ ) — the thymus and spleen were aseptically removed and observed (A); Thymus and spleen indexes; data were presented as means  $\pm$  standard error of mean.  $n=4$  per group (B). The thymus of control rats delineating compact histoarchitecture with normal lymphocyte (C, G). Arsenic-exposed thymus delineating lymphocyte-depleted areas (solid arrow) and innumerable pyknotic nuclei (white arrow head) (D, H). Black thick arrow indicating recovery in terms of cellular organisation and histoarchitecture of the thymus when L-AA and  $\alpha$ -T supplementation was given along with arsenic treatment (E, I). The thymus from only L-AA and  $\alpha$ -T supplemented group delineating normal histoarchitecture akin to that of the control (F, J). The spleen of control rat delineating normal splenic histoarchitecture (K, O). Arsenic-exposed spleen showed cellular-depleted areas (black broken arrow) around the central artery of germinal centre, interstitial fibrous tissue hyperplasia (white thick arrow), and reduction of white pulp area and expansion of red pulp area (L, P). The spleen from arsenic-treated rat supplemented with L-AA and  $\alpha$ -T delineating normal histoarchitecture and red pulp areas were reduced to normal range (M, Q); The spleen of only L-AA and  $\alpha$ -T supplemented group showing normal histomorphology akin to that of the control (N, R). C, cortex; M, medulla; RP, red pulp area; WP, white pulp area

spectrophotometrically after reacting with 2–4-DNPH to create 2–4-dinitrophenyl hydrazone derivatives (at acidic pH) [33, 35]. Following protein precipitation with equal volume of 20% trichloroacetic acid (TCA), precipitated proteins were resuspended with 2–4-DNPH (21% in 2N HCl) solution. After incubating the samples for 15–20 min at room temperature, the proteins were precipitated with 20% trichloroacetic acid before centrifugation at  $5700 \times g$  at  $4^\circ\text{C}$  [33, 35]. The proteins that precipitated were rinsed with an ethanol: ethyl acetate (1:1) solution before centrifugation at  $5700 \times g$  at  $4^\circ\text{C}$  [33]. Then the precipitate was resuspended in guanidine solution (6N) and the absorbance was measured at 370 nm spectrophotometrically (JASCO v-530, Tokyo, Japan) against blank sample (2 M HCl, distilled water). Tissue protein carbonyl content was determined as M/mg protein [33, 35, 44, 45].

### Total Protein Extraction from Tissue and Immunoblotting

Total protein of the thymus and spleen was isolated by homogenisation in ice cold RIPA lysis buffer (150 mM NaCl, 50 mM Tris, 0.5% sodium deoxycholate, 0.1% SDS, and 0.1% NP-40) containing complete EDTA-free protease inhibitor cocktail [33]. Protein concentration was determined by using the Bradford assay [33]. Identical sample concentration in laemmli sample buffer was put onto SDS–polyacrylamide. The electrophoresis was performed at fixed voltage of 60 V and the separated proteins from SDS–polyacrylamide gel were transferred onto polyvinylidene fluoride (PVDF) membrane (Immobilon®-P

PVDF Membrane, Millipore, Cat. No. IPVH00010) (activated with 100% methanol for 15–20 s, then transferred it to a petri dish of Milli-Q water for 2 min) for 2.5 h at 180 mA and blocked with 5% BSA for 2 h at  $25^\circ\text{C}$ . The blocked blots were washed thrice with Tris buffered saline, with 0.1% Tween-20 (TBS-T) for 15 min each. Blots were then probed with primary antibodies (Dilution 1:1000) against NF- $\kappa$ B, p-ERK, ERK, Bcl-2, Bax, Caspase-3, Nrf2, and  $\beta$ -actin overnight at  $4^\circ\text{C}$ . On 2nd day, blots were washed thrice with TBS-T for 15 min each and probed with alkaline phosphatase-conjugated secondary antibodies (dilution 1:1000) for 90 min at  $25^\circ\text{C}$ . Blots were then washed twice with TBS-T followed by washing once with alkaline phosphatase buffer (AP-Buffer). Immunoreactive proteins were spotted by using NBT-BCIP (nitro blue tetrazolium- 5-bromo-4-chloro-3-indolyl-phosphate) substrate solution. The band intensities were quantified by using Image-J software (Image-J; NIH, Bethesda, MD, USA). As a loading control,  $\beta$ -actin was employed [1, 33]. Three ( $n=3$ ) samples (biological triplicate) from each group were considered for immunoblotting for each protein.

### Immunohistochemistry

The thymus and spleen were washed in  $1 \times$  phosphate buffer solution (PBS) and fixed in 10% neutral buffered formalin for 48 h. Following dehydration, tissues were embedded in paraffin. Thin paraffin sections were obtained using a well precision rotary microtome (Leica biosystems). Tissue sections were deparaffinised, rehydrated with descending grades of ethanol. Following antigen retrieval using citrate buffer solution (pH 6), thin tissue sections were washed in  $1 \times$  phosphate buffer solution. Thereafter, tissue sections were blocked with 2% bovine serum albumin with 0.1% Tween 20 for 1 h. After blocking, tissue sections were incubated with the primary antibody for cleaved caspase-3 (Asp175) rabbit mAb (Cell Signaling Technology, Cat No. 9664) overnight at  $4^\circ\text{C}$ . Following incubation period, tissue sections were washed with  $1 \times$  phosphate buffer solution. Thereafter, these sections were incubated with alexa fluor<sup>TM</sup> 488 goat anti-rabbit secondary antibody for 2 h. Following a wash with  $1 \times$  PBS, the tissue slices were incubated with DAPI for 5 min. Next, tissue sections were washed with  $1 \times$  PBS and mounted with mounting media. Fluorescent images were obtained by using Leica confocal microscope with LasX software [46].

### Haematological Profiling

Complete blood count (CBC) and haemoglobin estimation were performed by using an automated cell counter (PCE-210, ERMA INC. Tokyo, Japan).

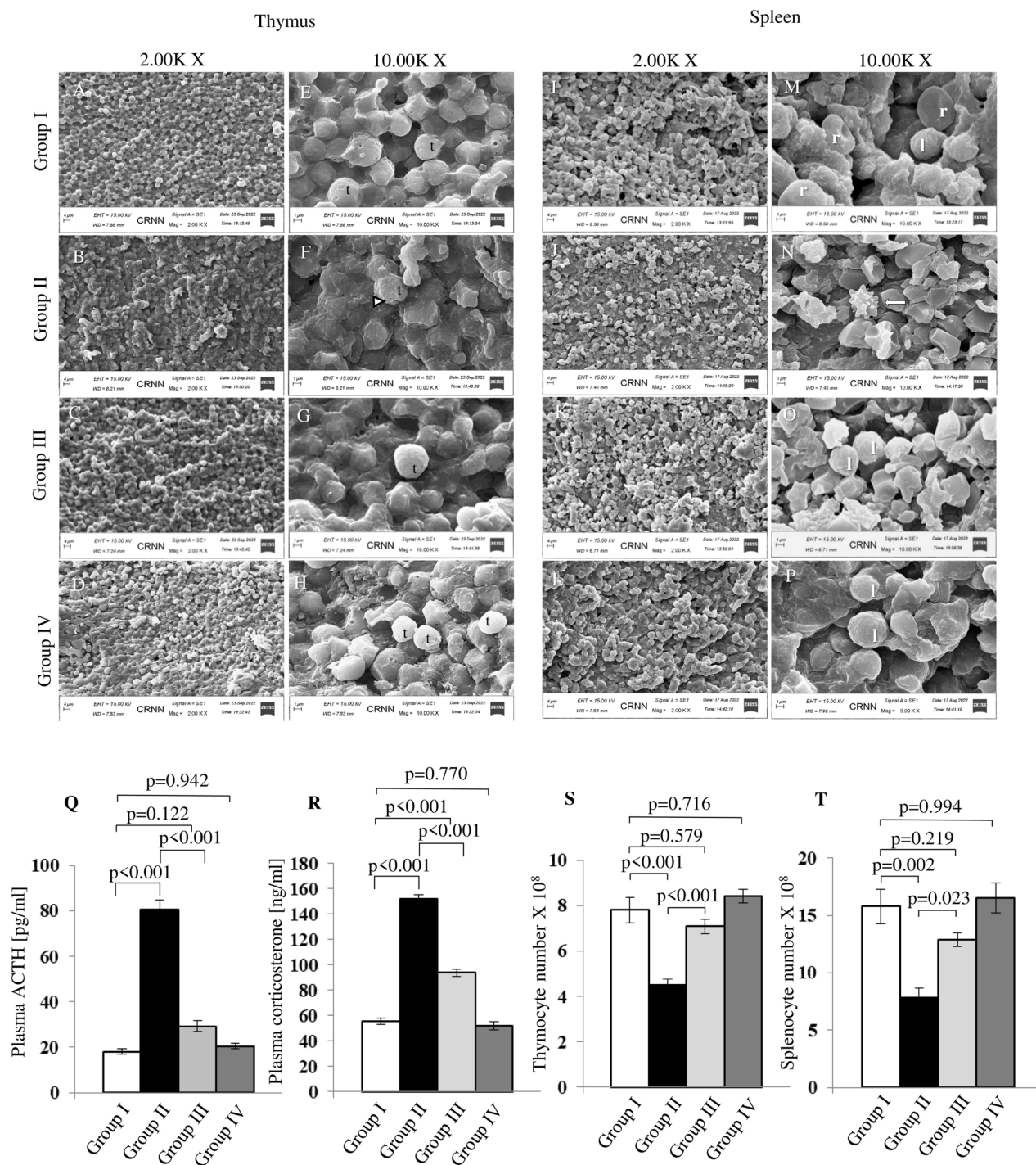


**Fig. 3** Effect of supplementation with L-AA and  $\alpha$ -T on arsenic-induced thymic and splenic injuries — scanning electron micrograph of control thymus delineating normal surface morphology of the thymus ( $n=3$ ) (A, E). Micrograph of arsenic-exposed thymus depicting loss of surface homogeneity and structural deformity of thymic tissues (B, F). L-AA and  $\alpha$ -T supplemented arsenic-exposed thymus depicting recovery of surface morphology towards normal (C, G). Micrograph of the thymus of only L-AA and  $\alpha$ -T supplemented rats showing normal surface topography akin to that of the control (D, H). SEM images of control spleen depicting normal surface morphology ( $n=3$ ) (I, M). The images of arsenic-treated rats depicting loss of surface homogeneity and echinocytes (white arrow) (J, N). Images

of the spleen from L-AA and  $\alpha$ -T supplemented arsenic-treated rat delineating recovery of surface morphology towards normal (K, O). The spleen of only L-AA and  $\alpha$ -T supplemented rat delineating normal surface topography (L, P). *t*, thymocyte; *r*, RBC; *l*, lymphocyte. The statistical graph depicting the effect of supplementation of L-AA and  $\alpha$ -T on arsenic-induced altered plasma ACTH and corticosterone levels (Q, R). The statistical graph delineating the impact of combined supplementation of L-AA and  $\alpha$ -T on arsenic-induced altered total thymocyte count and total splenocyte count in the thymus and spleen respectively (S, T). Data were presented as mean  $\pm$  (SEM) standard error of mean.  $n=4$



## Lymphocyte Isolation from Whole Blood

Collected blood was diluted with same volume of isotonic 1X PBS. Then the diluted blood was layered over Histo-paque-1077 in sterile conical tube and subjected to centrifugation at 3000 rpm for 15–20 min. After centrifugation, the plasma layer was carefully aspirated with Pasteur pipette. Then the opaque interface containing lymphocytes was transferred into a clean Eppendorf tube. Collected lymphocytes were washed with isotonic 1X PBS and subjected to downstream experiments.

## Quantification of Intracellular ROS Generation Within PBMCs

Intracellular ROS generation in peripheral blood mononuclear cells (PBMCs) was quantified by using the ROS sensitive fluorescence indicator DCFH-DA (2',7' dichlorodihydrofluorescein diacetate). DCFH-DA enters into the cell, where the acetyl-groups of DCFH-DA is cleaved off by cellular esterase to produce DCFH. In presence of ROS, DCFH is transformed into green fluorescence emitting DCF. Following the addition of 20  $\mu$ M DCFH-DA, the cell suspensions were incubated at 37 °C for 15 min. DCF fluorescence was measured at 530 nm using a FACS scan flow cytometer (BD FACS VERSE™, USA) and analysed using the BD FACSuite software (v1.0.5.3841).

## Detection of Cell Apoptosis by Flow-Cytometry

One hundred microliters of cell suspensions with  $1 \times 10^6$  cell concentration was incubated at room temperature for 15 min with 5  $\mu$ l of FITC-Annexin V and 10  $\mu$ l of propidium iodide (PI). The cell apoptosis was eventually analysed using a FACS scan flow cytometer (BD FACS VERSE™, USA) and BD FACSuite software (v1.0.5.3841).

## Single Cell Gel Electrophoresis Assay (COMET Assay)

Suspension of peripheral blood lymphocyte (100  $\mu$ l) was mixed with 100  $\mu$ l of 1% low melting point agarose (SRL, Cat. No.60645) and embedded onto the 1% normal melting point agarose (BIORON, Cat. No.604001) coated slide. These slides were immersed in chilled lysis solution (NaCl 1.2 M, Na<sub>2</sub>EDTA 100 mM, Sodium lauryl sarcosinate 0.1%, NaOH 0.26 M, pH13) and left in refrigerator (2–8 °C) overnight. In an alkaline environment, DNA was permitted to unwind [35]. Electrophoresis was carried out for 20 min at 280 mA and 20 V under alkaline conditions (NaOH 0.03 M, Na<sub>2</sub>EDTA 2 mM, pH 12.3) [35]. During electrophoresis, fragmented DNA migrates out from the nucleus, and migration is inversely related to fragment size [35]. These slides were neutralised using neutralising buffer before being

stained with the fluorescent dye ethidium bromide (2  $\mu$ g/ml) [35]. Image was taken using fluorescence microscopy (Zeiss, Thornwood, NY, USA). Comet tail length was measured in each gel. We measured the DNA damage manually in the CaspLab software.

## RNA Extraction from Peripheral Blood Leukocytes and Sequencing

Whole blood was treated with erythrocyte lysis buffer followed by centrifugation at 750 g for 10 min [47]. Then the cell pellet (leukocyte fraction) was washed with 1X PBS. Total RNA was extracted from all 8 samples ( $2 \times 4 = 8$ , each group consist 2 biological replicates) using PreAnalytiX PAXgene Blood RNA Kit (Cat. No. 762174). RNA samples were quantified using Qubit RNA BR assay. RNA integrity number (RIN) was measured using RNA screen Tapes. Enrichment of mRNAs was performed using oligo-dT containing magnetic beads (NEB, Cat. No. E7490L). After purification, cDNA was synthesised. A modified NEBnext RNA ultra II directional (NEB, Cat. No. E7760L) protocol was employed to construct the cDNA libraries for mRNA sequencing. Following that, the cDNA was transformed to double-stranded cDNA by substituting uracil for thymine. The double-stranded cDNA fragments were subjected to 3'end adenylation and adapter ligation. Prepared libraries were sequenced on illumina Novaseq V 1.5 instrument to generate 40 M, 150-bp paired end reads/sample. After generation of raw data, pre-processing of raw data was performed by removing adapter sequence and contamination sequence (using Trimmomatic Tool). Alignment of pre-processed data to rat reference genome was performed using HiSAT2. These filtered read counts were normalised in DESeq2, to assess gene expression levels.

## RNA-Sequencing Data Analysis

From the list of the differentially expressed genes (DEGs), we have considered those genes which were differentially expressed between group I vs group II and group II vs group III ( $p < 0.005$ ). A heatmap of significantly DEGs was constructed and clustering analysis was performed using iDEP.96 (South Dakota State University). KEGG (Kyoto Encyclopedia of Genes and Genomes) pathway and gene ontology (GO) enrichment analysis were performed on differentially expressed genes (DEGs) using iDEP.96 under FDR  $< 0.05$ . The weighted correlation network analysis (WGCNA) is a popular tool for co-expression analysis and was performed to find functionally interesting gene modules. Visualisation and network analysis was performed using STRING and candidate gene identification was performed using cytoHubba under cytoscape software in terms of degree centrality and shortest pathway.

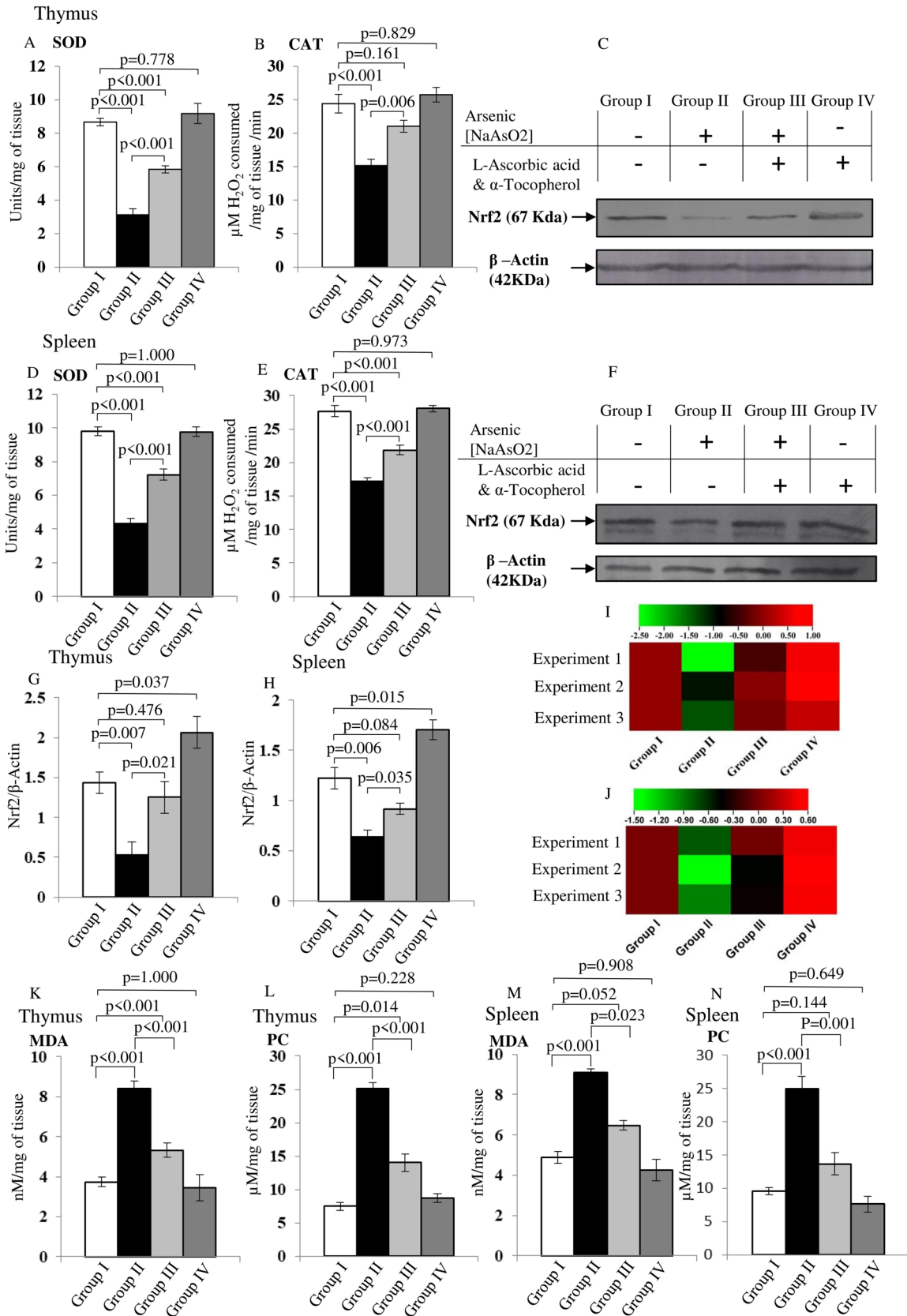


**Fig. 4** Effect of L-AA and  $\alpha$ -T on arsenic-induced oxidative stress in the thymus and spleen. The activity of (SOD) and (CAT) of the thymus and spleen of rats (A, B, D, E). Data were presented as mean  $\pm$  SEM (standard error of mean),  $n=4$  per group. Representative image of immunoblot of Nrf2 expression in the thymus (C) and spleen (F), where  $\beta$ -actin was used as the loading control. The band pixel intensity of Nrf2 of the thymus (G) and spleen (H) was standardised to that of the  $\beta$ -actin for each group. Each value was expressed as mean  $\pm$  SEM,  $n=3$  per group. The fold change of Nrf2 expression in respect to control in the thymus (I) and spleen (J) was expressed as heatmap. Non-enzymatic parameters of oxidative stress such as malondialdehyde (MDA) formation and protein carbonyl (PC) content in the thymus (K and L respectively) and spleen (M and N respectively) for each group. Each value was expressed as mean  $\pm$  SEM (standard error of mean),  $n=4$  per group

## Statistical Analysis

Each experimental group comprised of twelve adult male Wistar rats ( $n=12$  per group). Each experiment was performed in triplicate and the results are presented as mean  $\pm$  SEM. The statistical significance between the group mean values was measured by one-way analysis of variation (ANOVA) followed by Tukey's HSD post hoc test (SPSS 11.0; SPSS Inc., Chicago, IL, USA).  $p < 0.05$  was considered as statistically significant.

## Results

### Effect of L-AA and $\alpha$ -T Co-administration on Altered Thymus and Spleen Indexes due to Arsenic Exposure

There were no noteworthy differences in body weight along with other general parameters observed among the experimental animals in all the groups. However, arsenic exposure for 30 consecutive days decreased the size of the thymus and spleen (Fig. 2A). The thymus and spleen indexes in group II animals (arsenic-exposed group) were significantly lower than that of in group I ( $p < 0.001$  in both cases). Notably, in comparison to group II, upon co-administration of L-AA and  $\alpha$ -T after arsenic treatment led to significant increase in thymus and spleen indexes in group III ( $p < 0.001$  in both cases respectively) (Fig. 2B). However, there were no significant differences regarding thymus and spleen indexes between group I and group IV (Fig. 2B).

### Role of L-AA and $\alpha$ -T Co-administration on Altered Histomorphology of the Thymus and Spleen due to Arsenic Toxicity

Thymus sections from group I rats showed compact thymic morphology with numerous lymphocytes. Arsenic exposure caused marked disintegration in thymic

morphology including lymphocyte-depleted areas and innumerable pyknotic nuclei. Co-administration of L-AA and  $\alpha$ -T remarkably alleviated the anomalies caused by arsenic toxicity. No noticeable structural differences were observed between group I and group IV rats (Fig. 2C–J). Splenic histology of group I rats was characterised by compact splenic morphology with well-organised germinal centres. Arsenic treatment caused disintegration of the histoarchitecture of the spleen including expansion of the red pulp areas and hyperplasia of interstitial fibrous tissues. Upon co-administration of L-AA and  $\alpha$ -T, anomalies caused by arsenic treatment were absent and red pulp areas were reduced to a near normal range. Administration of only L-AA and  $\alpha$ -T showed the normal splenic histoarchitecture like group I rats (Fig. 2K–R).

### Effect of L-AA and $\alpha$ -T Co-administration on Arsenic-Induced Altered Surface Topography of the Thymus and Spleen

Studies using scanning electron microscopy showed compact thymic surface morphology with a dense population of round-shaped thymocytes in group I rats. Arsenic exposure led to an increase in surface deformity of the structural organisation of thymic tissues including the loss of thymocytes compared to that of the group I rats. In comparison to group II rats, surface morphology of the thymus was returned to normal in group III rats. Application of only L-AA and  $\alpha$ -T depicted normal surface morphology of the thymus like that of group I (Fig. 3A–H).

In comparison to group I, the spleen of group II rats showed a loss of surface homogeneity, presence of echinocytes, and loss of lymphocytes. By contrast, administration of L-AA and  $\alpha$ -T led to recovery of surface morphology towards normal. No noticeable changes were observed between group I and group IV rats (Fig. 3I–P).

### Effect of Co-administration with L-AA and $\alpha$ -T on Arsenic-Induced Alteration of Plasma ACTH and Corticosterone Level

Arsenic exposure (group II) led to a significant ( $p < 0.001$ ) increase in plasma ACTH and corticosterone levels, as compared to the group I rats (Fig. 3Q–R). Upon co-administration of L-AA and  $\alpha$ -T in arsenic-exposed rats (group III), the plasma ACTH and corticosterone levels were significantly restored ( $p < 0.001$  in both cases), but a significant ( $p < 0.001$ ) difference regarding the plasma corticosterone level between group I and group III rats was also noted. No significant alteration was observed between group I and group IV rats.

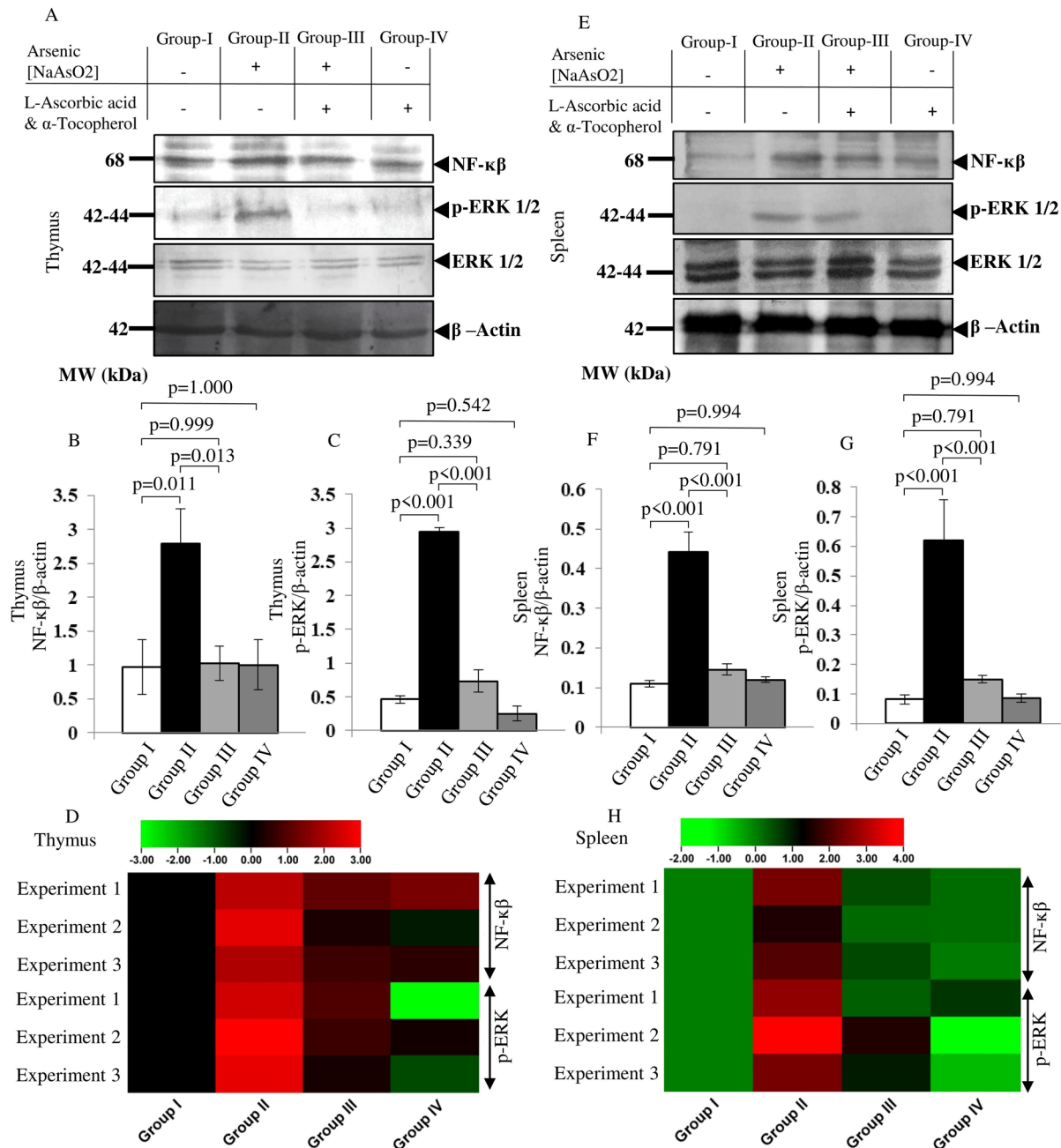


**Fig. 5** Effect of L-AA and  $\alpha$ -T on arsenic-induced inflammation in the thymus and spleen. Immunoblots of NF- $\kappa$ B, p-ERK, and total ERK from the thymus (A) and spleen (E).  $\beta$ -actin was used as the loading control. The band pixel intensity NF- $\kappa$ B and p-ERK from the thymus (B, C) and spleen (F, G) were standardised to that of the

$\beta$ -actin for each group. Each value was expressed as mean  $\pm$  standard error of mean.  $n = 3$  per group. The fold change of NF- $\kappa$ B and p-ERK expression in respect to control in the thymus (D) and spleen (H) was expressed as heatmap

### Effect of Co-administration of L-AA and $\alpha$ -T on Arsenic-Mediated Alteration of Total Thymocyte Count and Splenocyte Count

In comparison to group I, arsenic treatment led to a marked decrease in total thymocyte and splenocyte counts of the thymus and spleen respectively ( $p < 0.001$ ,

$p < 0.01$  respectively). Co-administration of L-AA and  $\alpha$ -T showed significant restoration of both thymocyte and splenocyte counts in arsenic-exposed rat ( $p < 0.001$ ,  $p = 0.0023$  respectively). However, no significant difference was observed between group I and group IV rats (Fig. 3S and T).

### Effect of Co-administration of L-AA and $\alpha$ -T on Arsenic-Mediated Oxidative Stress in the Thymus and Spleen

When treated with sodium arsenite, the oxidative stress markers were seen to be altered both in the thymus and spleen of group II rats. In comparison to the control, SOD and CAT activities of the thymus and spleen were markedly decreased ( $p < 0.001$  in both cases for SOD and CAT) in group II rats. In comparison to group II, SOD and CAT activities of the thymus ( $p < 0.001$  and  $p = 0.006$  respectively) and spleen ( $p < 0.001$  for both cases) were significantly improved in group III rats (Fig. 4A–B and 4D–E). However, no noteworthy alterations were observed in between group I and group IV rats.

Upregulation of Nrf2 (a transcription factor accountable for regulation of ARE-dependent genes expression) protects cells from the inimical effect of oxidative stress. As opposed to group I, group II rats had significantly lower level of Nrf2 in the thymus and spleen ( $p = 0.007$  and  $p = 0.006$  respectively). Co-administration of L-AA and  $\alpha$ -T (group III) significantly elevated the expression of Nrf2 in the thymus ( $p = 0.021$ ) and spleen ( $p = 0.035$ ), when compared to that of the group II rats. Strikingly, in comparison to group I, only co-administration of L-AA and  $\alpha$ -T appreciably enhanced the expression of Nrf2 in the thymus and spleen ( $p = 0.0037$  and  $0.015$  respectively) (Fig. 4F–J).

On the other hand, in comparison to group I, group II rats had increased levels of MDA and PC content in the thymus and spleen ( $p < 0.001$  in both cases for MDA and PC content). Meanwhile, L-AA and  $\alpha$ -T co-administration significantly reduced the MDA and PC content in the thymus ( $p < 0.001$  in both cases) and spleen ( $p = 0.023$  and  $p < 0.001$  respectively) of group III rats when compared with that of group II rats (Fig. 4K–N). However, no significant difference was observed between group I and group IV rats.

### Role of L-AA and $\alpha$ -T Co-administration on Arsenic-Induced Alteration of NF- $\kappa$ B Expression and Phosphorylation of ERK

NF- $\kappa$ B is a crucial transcription factor that is activated by oxidative stress and is also involved in inflammation. The expression of NF- $\kappa$ B was markedly upregulated in the thymus and spleen of group II rats ( $p = 0.011$ ,  $p < 0.001$  respectively), when compared to that of group I. Along with this, arsenic exposure strongly induced phosphorylation of ERK in the thymus and spleen ( $p < 0.001$  in both cases). L-AA and  $\alpha$ -T co-administration relatively maintained them at lower level in group III rats. Only administration of L-AA and  $\alpha$ -T did not exert any noticeable difference with group I rats (Fig. 5A–H).

### Effect of Co-administration of L-AA and $\alpha$ -T on Arsenic-Induced Alteration of Bcl-2, Bax, and Cleaved-Caspase-3 Expression in the Thymus and Spleen

In comparison to group I, the expression of Bcl-2 in the thymus and spleen of group II rats was markedly downregulated ( $p = 0.001$  and  $p = 0.005$  respectively). By contrast, Bax and cleaved caspase-3 expression was significantly upregulated in the thymus ( $p < 0.001$  for both cases) and spleen ( $p < 0.001$  and  $p < 0.001$  respectively) of group II rats. Following administration of L-AA and  $\alpha$ -T, it was seen that the expression of Bcl2, Bax, and cleaved caspase-3 returned to near normal level in the thymus ( $p = 0.014$ ,  $p < 0.001$ , and  $p < 0.001$  respectively) and spleen ( $p = 0.030$ ,  $p < 0.001$ , and  $p < 0.001$  respectively) in group III rats. No noteworthy variation was noted between group I and group IV rats in all cases (Figs. 6A–L and 7).

### Effect of L-AA and $\alpha$ -T Co-administration on Erythrocyte, Lymphocyte, and Total Leukocyte Counts of Adult Male Rats Under Arsenic-Exposed State

As opposed to group I, erythrocyte, total leukocyte, and lymphocyte counts along with haemoglobin concentration were significantly decreased in group II rats ( $p < 0.001$  for erythrocyte count, total leukocyte count and total lymphocyte count and  $p = 0.002$  for Hb concentration) compared to those in group I rats. Following co-administration of L-AA and  $\alpha$ -T, counts of erythrocyte, lymphocyte, and total leukocyte and haemoglobin concentration were significantly restored towards normal in group III rats ( $p < 0.001$ ,  $p = 0.012$ ,  $p < 0.001$  and  $p = 0.038$  respectively). Meanwhile, a significant difference still existed in between group I and group III regarding total leukocyte and lymphocyte counts and haemoglobin concentration ( $p = 0.040$ ,  $p = 0.050$ , and  $p = 0.0314$  respectively). However, there was no significant alteration in between group I and group IV in all the cases (Fig. 8A–D).

### Impact of L-AA and $\alpha$ -T Co-administration on Arsenic-Induced Reactive Oxygen Species Generation in Circulating Lymphocytes

Arsenic exposure resulted noteworthy increase ( $p < 0.001$ ) in the generation of reactive oxygen species in circulating lymphocytes of group II rats compared to that of group I rats. Following co-administration of L-AA and  $\alpha$ -T (group III), reactive oxygen species generation was significantly reduced ( $p < 0.001$ ) in circulating lymphocytes as compared with group II. There was no noticeable variation between group I and group IV rats (Fig. 8E–I).

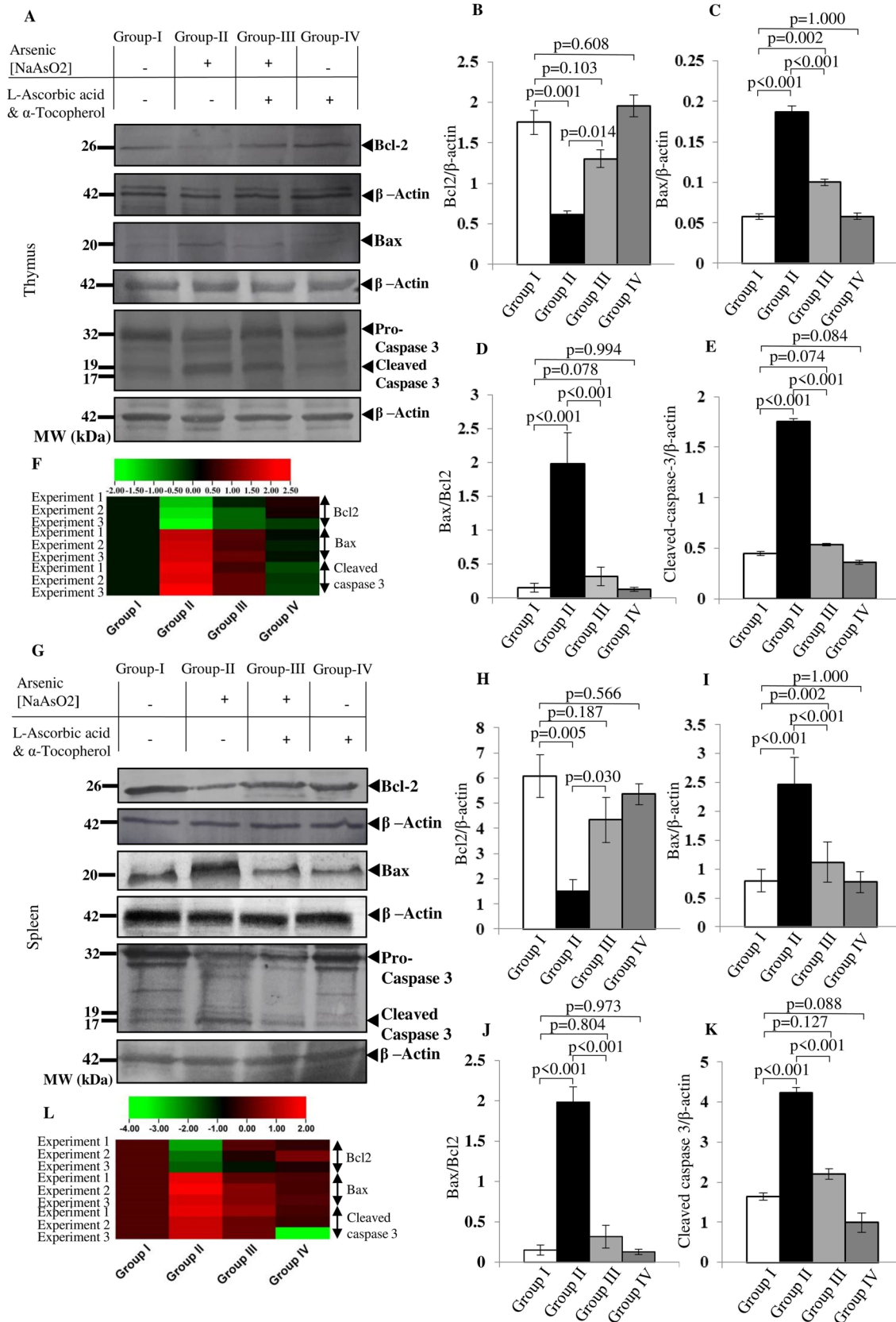


**Fig. 6** Impact of L-AA and  $\alpha$ -T on arsenic-induced activation of intrinsic apoptosis pathway in the thymus and spleen. Immunoblots of Bcl2, Bax, and cleaved-caspase-3 from the thymus (A) and spleen (F).  $\beta$ -actin was used as the loading control. The band pixel intensity of Bcl2, Bax, and cleaved caspase-3 from the thymus (B–E) and spleen (G–J) was standardised to that of the  $\beta$ -actin for each group. Each value was expressed as mean  $\pm$  SEM.  $n=3$  per group. The fold change of Bcl2, Bax, and cleaved caspase 3 expression in respect to control in the thymus (K) and spleen (L) was expressed as heatmap

### Effect of L-AA and $\alpha$ -T Co-administration on Arsenic-Induced Apoptotic Death of Lymphocytes

The apoptotic effects of inorganic arsenic and its possible prevention by co-administration of L-AA and  $\alpha$ -T were evaluated by flowcytometry analysis following staining with FITC conjugated annexin V and propidium iodide. FITC-conjugated annexin V is detectable in both early and late phases of apoptosis, while propidium iodide is only detectable in late apoptosis or necrosis. As shown in Fig. 8J–O, treatment with arsenic led to significant reduction in percentage of live lymphocyte ( $p < 0.001$ ) and concomitant increase in the percentage of apoptotic lymphocyte ( $p < 0.001$ ), as compared to group I. In addition, the percentage of live lymphocyte was significantly increased while the percentage of apoptotic lymphocyte was significantly decreased in group III rats as compared to group II. No noteworthy difference was observed between group I and group IV rats.

### Effect of L-AA and $\alpha$ -T Co-administration on Arsenic-Induced DNA Damage of Lymphocytes

In order to measure the oxidative DNA damage of circulating lymphocytes in each group, the percentage of tail DNA and olive tail moment were quantified in each gel. As shown in Fig. 9, in comparison to the control group, the arsenic-treated group had higher percentage of tail DNA ( $p < 0.001$ ) and olive tail moment ( $p < 0.001$ ). Co-administration of L-AA and  $\alpha$ -T significantly reduced the tail DNA percentage ( $p < 0.001$ ) and olive tail moment ( $p < 0.001$ ) in circulating lymphocytes in group III rats compared to group II rats. But there was still a significant difference in tail DNA percentage ( $p < 0.001$ ) and olive tail moment ( $p = 0.014$ ) between group I and group III rats. No noticeable difference was observed between group I and group IV rats.

### Transcriptome Characterisation of Circulating Leukocytes Induced by L-AA and $\alpha$ -T Co-administration Under Arsenic-Exposed Condition

We have taken into account the genes that were differentially expressed in between group I vs group II and group II

vs group III ( $p < 0.005$ ). From this screening, we got sixty-seven (67) DEGs. To better understand the impact of L-AA and  $\alpha$ -T co-administration on arsenic-exposed leukocytes, 67 significantly ( $p < 0.005$ ) differentially expressed genes (Fig. 10A) were further clustered into four clusters (cluster A = 17 genes, cluster B = 30 genes, cluster C = 16 genes, cluster D = 4 genes) (Fig. 10D). KEGG pathway analysis of screened DEGs revealed that those genes were primarily associated with glycerophospholipid metabolism, endocytosis, lysine degradation, haematopoietic cell lineage, leishmaniasis, and leukocyte trans-endothelial migration (Fig. 11A). GO term for biological processes also indicated that these screened DEGs were associated with leukocyte adhesion to vascular endothelial cells, leukocyte migration involved in the inflammatory response, positive regulation of cell motility, and leukocyte migration (Fig. 11B). WGCNA was used to find gene clusters (modules) with significantly correlated expression patterns with a threshold of 0.75 (Fig. 12A and B). From all experimental groups, one module (turquoise module) was identified. KEGG pathway of this turquoise module with 47 genes was enriched for tuberculosis, leukocyte trans-endothelial migration, and vitamin digestion and absorption (Fig. 12C).

STRING and cytoHubba were used to identify gene cluster with strongly correlated expression patterns in order to find an integrative network. From this analysis, it has been identified that Itga4, Itgam, MMP9, Rab5C, and Flt4 were the closely associated genes within PPI (protein–protein interaction) network in terms of degree centrality and shortest pathway (Fig. 12D and E). Most of these genes were involved in trans-endothelial migration. As shown in Fig. 10A, the expression of MMP9, Itga4, and Itgam significantly increased in leukocytes of group II rats, when compared to that of group I rats. By contrast, co-administration of L-AA and  $\alpha$ -T along with arsenic maintained them at lower level. There is no significant difference in terms of MMP9, Itgam, and Itga4 expression between group I and group IV.

## Discussion

Although arsenic exerts its anti-tumour and anti-cancer effects by suppressing Akt and MAPK oncogenic signalling pathways, but its therapeutic application is restricted due to its immunotoxic potential, which jeopardises the immune system in various ways. This investigation has shown that the co-administration of L-AA and  $\alpha$ -T alleviates arsenic-induced structure–function alterations of immune system.

In this study, arsenic-treated rats had decreased size and index of the thymus and spleen. The indexes of the immune organ/s are often used to assess the overall immune function of the body [48]. The decreased thymic and splenic indexes,

as observed in our study, are an indication of immunosuppression due to arsenic treatment. It may be due to arsenic-induced apoptosis, reduction in absolute B cell and T cell counts, alteration of the epigenetic landscape throughout the genome, inhibition of the lymphocyte stimulation, and suppression of its proliferation [49–52]. In accordance with these findings, we showed that arsenic caused gross disintegration of the histoarchitecture of the thymus and spleen. Areas of lymphocyte depletion, appearance of innumerable pyknotic nuclei, and dilated sinusoids were evident within the thymus of arsenic-exposed rats. Moreover, sclerosis and hyalinosis of the central artery of the germinal centre, reduction in white pulp size, and interstitial fibrous tissue hyperplasia were observed within the spleen. Loss of surface homogeneity and membrane blebbing on the surface of the thymic cells indicated the deleterious changes triggered by arsenic, as observed by scanning electron microscopy (SEM). SEM images of arsenic affected spleen depicted massive alteration of the surface morphology including loss of surface homogeneity, appearance of apoptotic bodies, and echinocytes. In our study, it was shown that L-AA and  $\alpha$ -T co-administration ameliorated the arsenic-induced anomalies, possibly due to maintenance of the structural integrity of the thymus, spleen, and mitotic activity of lymphocytes by L-AA [53, 54] and  $\alpha$ -T induced proliferation of thymic lymphocytes possibly by promoting T cell differentiation within the thymus [55].

Elevated plasma ACTH along with plasma corticosterone in arsenic-exposed rats reflected a state of arsenic-induced stress condition. Probably, it was due to crumbling of negative feedback mechanism of the HPA (hypothalamus-pituitary-adrenaline) axis. As per an earlier report, hippocampal damage was seen due to arsenic exposure which contributed to the breakdown of negative feedback mechanism of the HPA axis [29]. In addition to hypothalamus, hippocampus was shown to play an important role in maintaining negative tone over the HPA axis. Neural fibre tracts of fimbria-fornix contributed indispensable inhibitory communication conduit from hippocampus to hypothalamus [56]. This elevated plasma corticosterone level led to reduction of absolute thymocyte and splenocyte counts in the thymus and spleen respectively. It had been documented that elevated plasma corticosterone level led to thymic involution in Sprague–Dawley mice [31] and splenic involution in Wistar-Kyoto rats [32]. These reports further attest to our results shown in Fig. 2A that thymus and spleen indexes are affected on arsenic exposure in Wistar rats. It may be due to elevated corticosterone-induced apoptosis of CD4<sup>+</sup> and CD8<sup>+</sup> T cells by increasing the expression of endonucleases [30]. Corticosterone acts through glucocorticoid receptor (GR) within the cell. Löwenberg et al. [57] showed that unligand GR was required for T cell receptor (TCR) signalling. GR is a component of the multiprotein TCR complex which

also includes  $\Theta$ TCR chain, HSP-90 (Heat shock protein 90), FYN kinases, Lck kinase, and Zap-70 kinase [57, 58]. It was shown that GR-mediated signalling pathway was involved in thymic lymphocyte selection process. One related research having in vitro experiment revealed that TCR signalling can inhibit glucocorticoid-induced apoptosis whereas glucocorticoid treatment reduced TCR induce apoptosis [59]. GR and TCR signalling pathways neutralised each other in developing thymocytes expressing TCR with low or modest affinity towards self-peptide resulting in cell survival [59]. Increased plasma corticosterone caused the recruitment of GR in GR-mediated signalling pathway. Profound GR-mediated signalling leads to apoptosis of thymic lymphocytes [59]. In this present study, co-administration of L-AA and  $\alpha$ -T restored absolute thymocyte and splenocyte counts by reducing elevated plasma corticosterone level towards normal.

Zhang et al. (2021) showed that ascorbic acid (200 mg/kg) administration caused increased expression of Nrf2 in hippocampus and subsequently increased expression of SOD anti-oxidant enzyme and enhanced HO-1 expression to suppress the inflammatory response [60]. Previously, it was shown that in guinea pigs, deprivation of ascorbic acid lowered the number of hippocampal neurons [61]. Earlier studies reported that hippocampal neurons were protected from lead (Pb)-induced neurotoxicity by ascorbic acid supplementation [62, 63]. On the other hand,  $\alpha$ -tocopherol exhibited strong mitigation against pilocarpine-induced damages in the rat hippocampus [64] by improving mitochondrial dysfunction [65]. Mahmoud et al. reported that there was a negative correlation between plasma ascorbic acid and plasma corticosterone levels [66]. It was also reported that supplementation with  $\alpha$ -tocopherol reduced plasma ACTH and corticosterone levels in stress-induced Sprague–Dawley rats [67]. Therefore, it can be said that co-administration of L-ascorbic and  $\alpha$ -tocopherol restored plasma corticosterone levels to normal by reestablishment of negative feedback mechanism of HPA axis by improving hippocampal health in arsenic-exposed rats.

Under normal physiological conditions, an intricate antioxidant defence system is involved in ROS scavenging. The principal players in this antioxidant defence mechanism are SOD and CAT. SOD, which converts superoxide radicals to hydrogen peroxide and oxygen, is considered to be the body's first line of defence against the detrimental effects of superoxide ions. In contrast, catalase aids in the removal of hydrogen peroxide by converting it into water. Arsenic treatment led to excessive ROS generation in the thymus and spleen by limiting the activity of SOD and CAT. In comparison to control, the SOD and CAT activities were significantly decreased and MDA and PC contents were dramatically increased in the thymus and spleen of arsenic-treated rats. MDA is one of the primary products in ROS-induced lipid peroxidation and the PC content is a quantitative



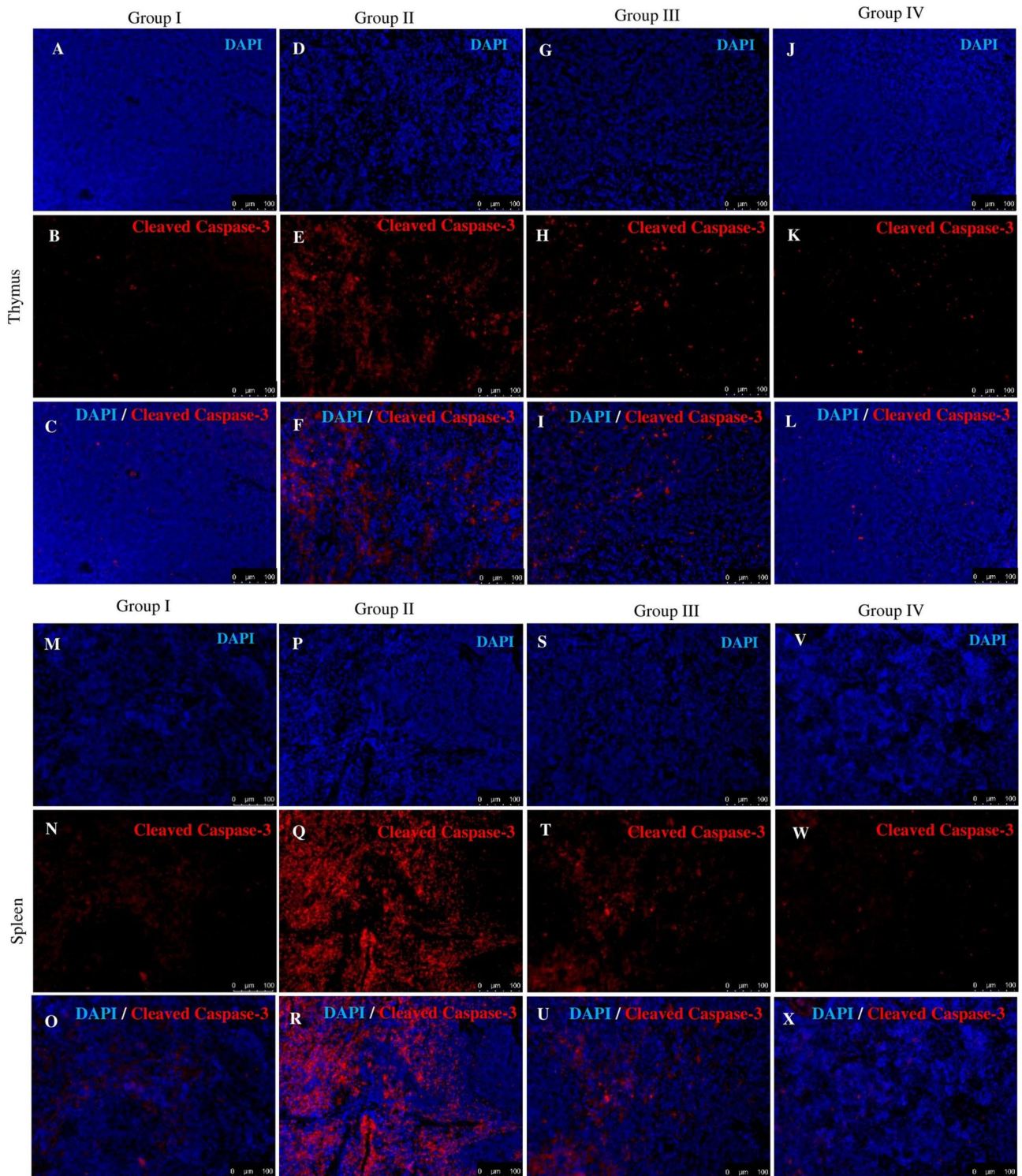


**Fig. 7** Immunohistochemistry of the thymus and splenic section was performed for cleaved caspase-3 staining. 1st row of 1st panel — nucleus stained with DAPI (A, D, G, J). 2nd row of 1st panel — cleaved caspase (red) (B, E, H, K). 3rd row of 1st panel — merged image of nucleus stained with DAPI and cleaved caspase 3 (C, F,

I, L). 1st row of 2nd panel — nucleus stained with DAPI (M, P, S, V). 2nd row of 2nd panel — cleaved caspase (red) (N, Q, T, W). 3rd row of 2nd panel — merged image of nucleus stained with DAPI and cleaved caspase 3 (O, R, U, X)

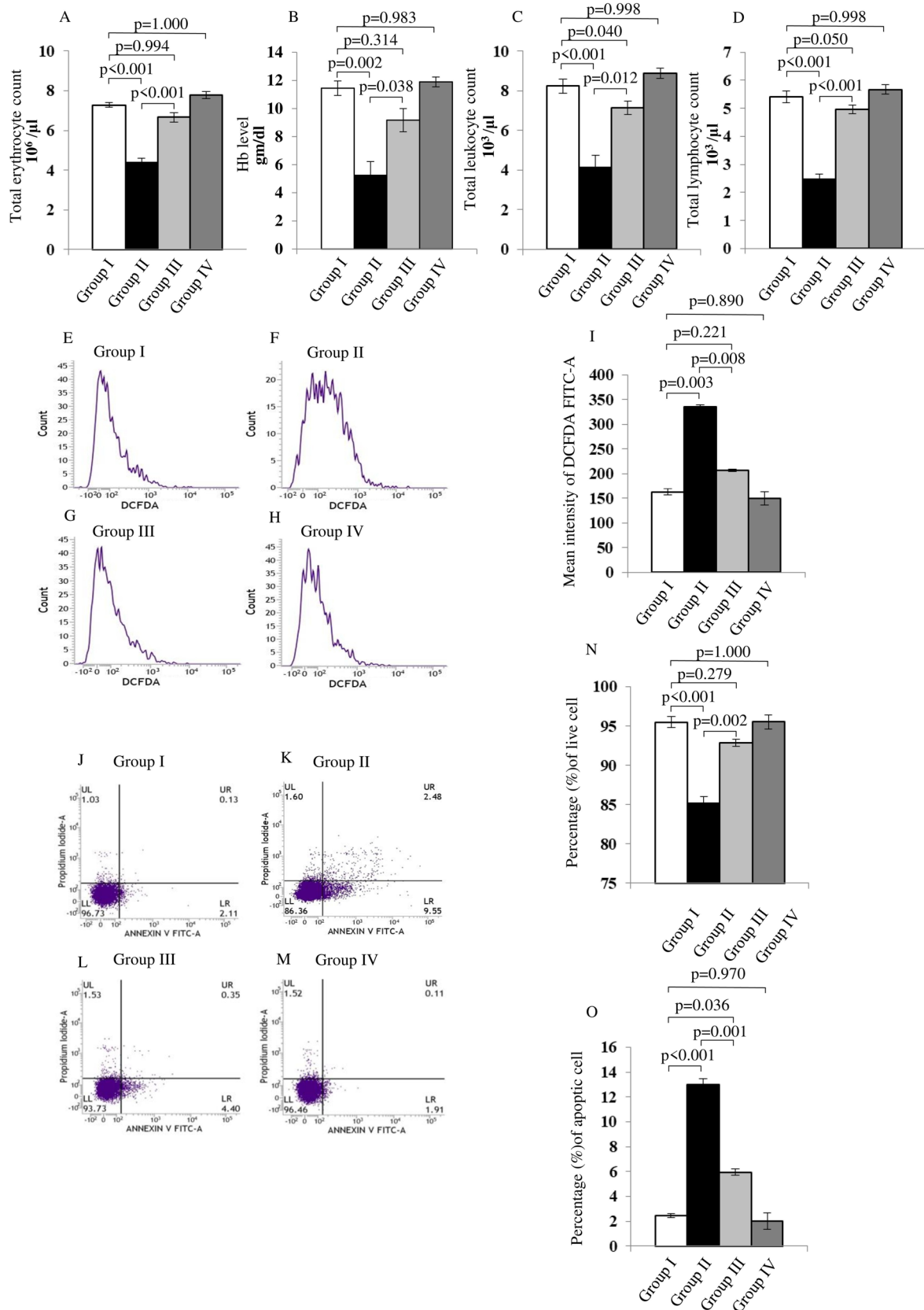


**Fig. 8** Ameliorative potential of combined supplementation with L-AA and  $\alpha$ -T on arsenic-induced alteration of haematological parameters and ROS-induced apoptosis of lymphocytes: total erythrocyte count (A), haemoglobin concentration (B), total leukocyte count (C), total lymphocyte count (D). Histogram plot of DCF fluorescence of lymphocytes (E–H). Mean intensity of DCFDA FITC-A of all group (I). Representative scatter plots of lymphocytes of each group stained with FITC-conjugated annexin V and propidium iodide (J–M). Percentage (%) of live cells (N) and apoptotic cell (O) for each group. Each value was expressed as mean  $\pm$  SEM.  $n=3$  per group

measure of the ROS-induced oxidation of amino acids in cellular proteins. In this study, it has been shown that arsenic exposure led to downregulation of Nrf2 expression at protein level in arsenic-exposed thymus and spleen. It may be due to arsenic-mediated global methylation [68]. One recent report showed that arsenic trioxide caused decrease in Nrf2 expression in the rat kidney [69]. This report attests to our result shown in Fig. 4C and Fig. 4F–I. Nrf2 regulates the expression of ARE-dependent genes to regulate the cellular anti-oxidant defence system against oxidative insult. In the presence of oxidative stress, Nrf2 dissociates from KEAP-1 cytosolic protein and translocates to the nucleus where it heterodimerises with Maf and binds to the ARE in the promoter site of the different anti-oxidant genes [70, 71]. Co-administration of L-AA and  $\alpha$ -T dramatically upregulated thymic and splenic Nrf2 expression in arsenic-exposed rats. In 2020, Li–Li Xu et al. reported that high dose of ascorbic acid mitigated pancreatic damage through Nrf2-mediated pathway in acute pancreatitis rat model [72]. Another related study showed that  $\alpha$ -tocopherol treatment markedly upregulated Nrf2 expression in ARDE-19 cell line [73]. In 2018, Vineetha et al. also showed that co-administration of L-AA and  $\alpha$ -T attenuated  $As_2O_3$ -mediated oxidative stress in H9c2 cardiomyocytes in in vitro system [74]. Therefore, it can be hypothesised that arsenic treatment disrupts the anti-oxidant defence mechanism by reducing the expression of Nrf2 and L-AA and  $\alpha$ -T co-administration can effectively neutralise the oxidative stress within the thymus and spleen by enhancing Nrf2 expression at protein level.

Oxidative stress seems to be involved in the activation of MAPKs, which include ERK1/2, P-38, and JNK1/2 [75]. Phosphorylation of MAPKs leads to the activation of NF- $\kappa$ B, which is an inflammatory transcription factor, involved in the regulation of pro-inflammatory cytokine production [1]. Arsenic has been shown to cause inflammation in rat [76] and human [77]. As shown in this study, we observed that arsenic exposure led to increased phosphorylation of ERK and a noteworthy elevation of NF- $\kappa$ B expression in both the thymus and spleen. Duan et al. showed that acute arsenic toxicity led to increased phosphorylation of ERK and expression of NF- $\kappa$ B in the thymus and spleen of C57BL/6 mice [1]. On the other hand, Yan et al. found that chronic arsenic exposure caused enhanced phosphorylation of ERK

and NF- $\kappa$ B expression in the spleen of kuming mice [27]. These reports further attest to our results shown in Fig. 5. We found that co-administration of L-AA and  $\alpha$ -T led to maintain the phosphorylation of ERK and NF- $\kappa$ B expression at low levels in arsenic-exposed rats. It may be due to ascorbic acid-induced inhibition of PKM2 expression [78].

The downregulation of Bcl2 expression and increased expression of Bax seems to be involved in the oxidative stress-induced apoptosis [79]. Bcl2 is an anti-apoptotic protein which is connected to the outer membrane of the mitochondria through its hydrophobic-carboxy terminal domain. Apoptogenic factor would normally be released from the mitochondria as a result of Bax/Bak oligomerisation. Bcl2 appears to prevent apoptosis by maintaining the integrity of the mitochondrial membrane by preventing the oligomerisation of Bax (pro-apoptotic protein) [80]. In this present work, we found that Bcl2 expression was dramatically reduced while Bax expression was significantly raised in arsenic-exposed thymus and spleen with subsequently enhanced expression of cleaved caspase-3, which indicated the activation of intrinsic apoptosis pathway. This data is consistent with some other recent reports showing downregulation of Bcl2 and upregulation of Bax expression in the uterus [33], thymus, spleen [23], and kidney [69] following the arsenic insult. Upon co-administration of L-AA and  $\alpha$ -T with arsenic treatment dramatically increased the expression of Bcl-2 and decreased the expression of Bax, which indicated that co-administration of L-AA and  $\alpha$ -T led to abrogate this arsenic-induced activated intrinsic apoptosis pathway in the thymus and spleen.

Haematological parameters delineated that total leukocyte count and total lymphocyte count were observed to reduce significantly, when compared with that of the unexposed one. It has been reported that arsenic caused suppression of stimulation and proliferation of lymphocytes [51]. Arsenic toxicity in rat also reduced the weight and cellularity of the thymus and spleen, which are the maturation site of T-lymphocytes and the proliferation site of B lymphocytes respectively [81]. According to the reports, arsenic had been positively linked with the apoptosis of plasma cell and lowered peripheral T lymphocyte [82, 83]. Thus, it is plausible to hypothesise that the decline in total leukocyte and lymphocyte count is caused by apoptosis of lymphocytes following the arsenic insult. In this present study, it has been shown that arsenic caused apoptosis of lymphocytes due to ROS-induced oxidative DNA damage. 8-oxoguanine is the principal oxidised base in DNA during oxidative damage of genomic DNA. In mammals, 8-oxoguanine DNA glycosylase-1 (8OGG1) is the major glycosylase, essential for the removal of 8-oxoguanine from DNA [84–86]. In the A549 cell line, micromolar dosages of arsenite reduced mRNA expression and enzymatic activity of 8OGG1 [87]. Apart from this, apyrimidinic/apurinic endonuclease 1 (APE1)

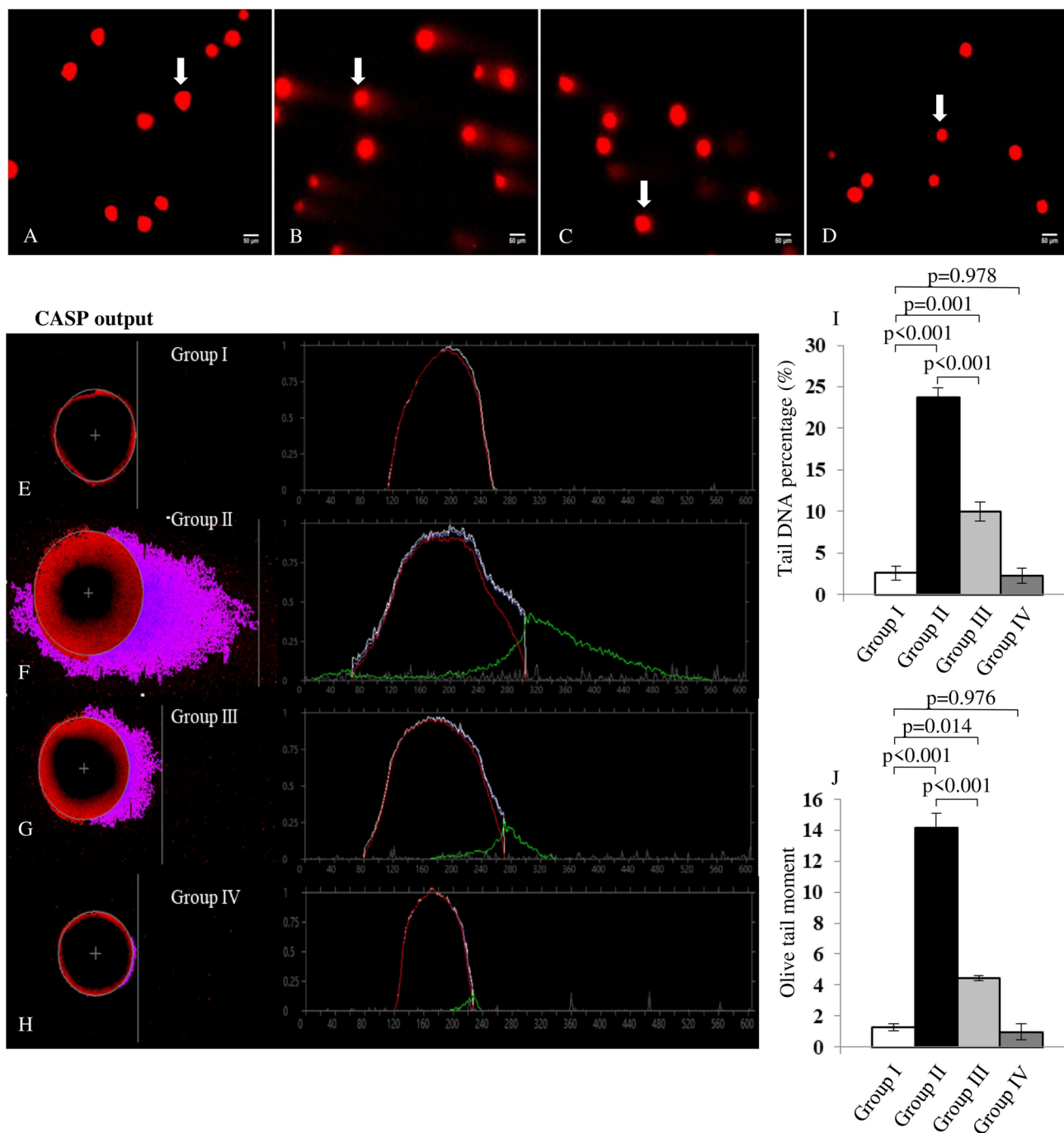


**Fig. 9** Effect of supplementation with L-AA and  $\alpha$ -T on arsenic-induced DNA disintegration of circulating lymphocytes — representative image of single cell gel electrophoresis (COMET assay) of DNA of circulating lymphocytes of each group (A–D). Representa-

tive CASP output of each group, red lines represent the head of the COMET and green lines represent the tail of the COMET (E–H). Tail DNA % (I) and olive tail moment (J) of each group. Each value was expressed as mean  $\pm$  standard error of mean.  $n = 3$  per group

was shown to be diminished at the mRNA and protein level following the arsenic insult [88]. It has also been reported that, the mRNA of DNA polymerase  $\beta$  was downregulated, following the arsenic treatment [89]. In 2003, Andrew et al. reported that arsenic-defiled drinking water was found to be

negatively linked with expression of XPF, XPB, and ERCC1 genes in lymphocyte [90]. In 2007, Kadirvel et al. showed that arsenic led to inhibition of the DNA repair mechanism by inducing ROS-mediated augmentation of DNA–protein cross-link due to carbonylation of the protein [91]. While

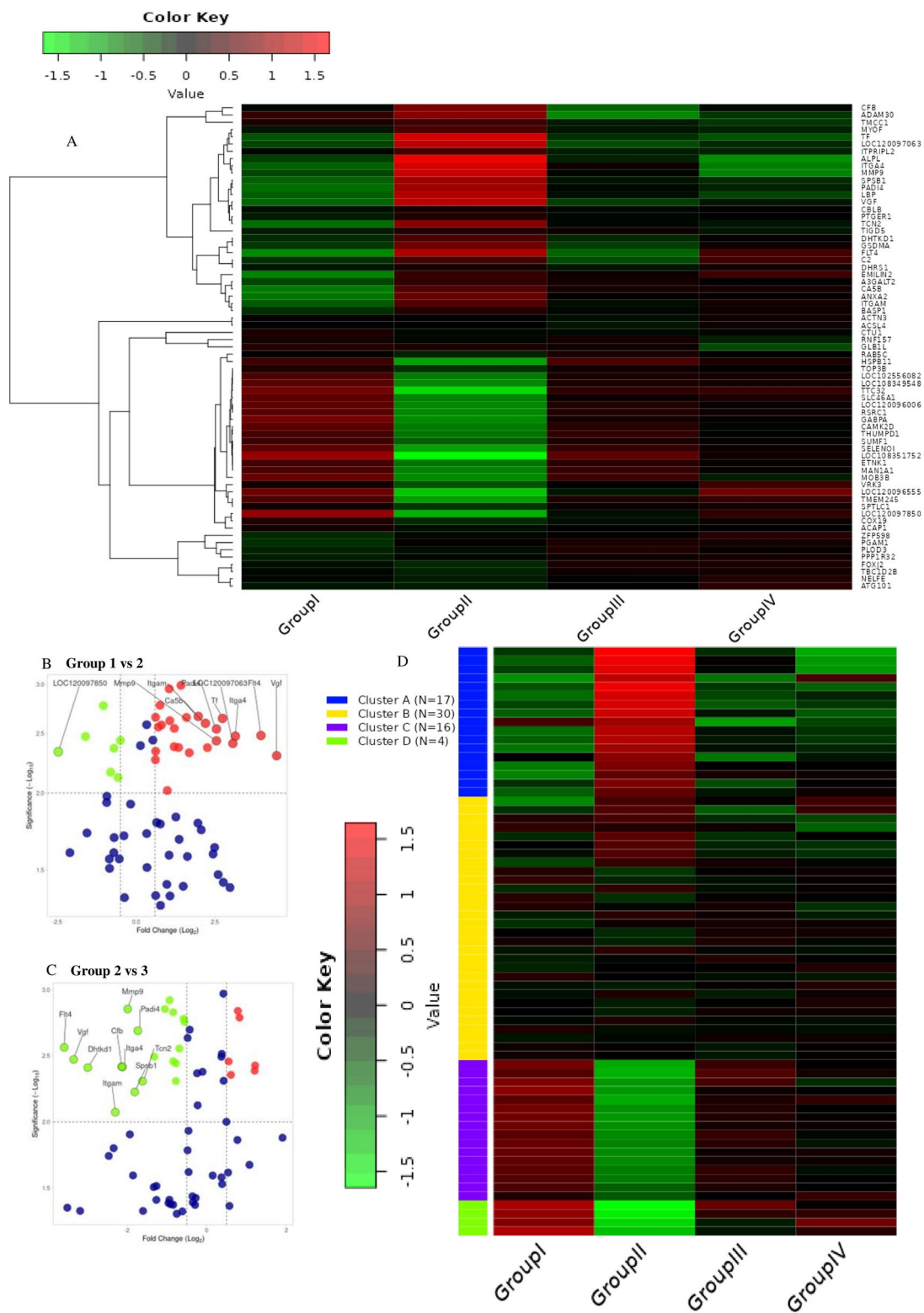
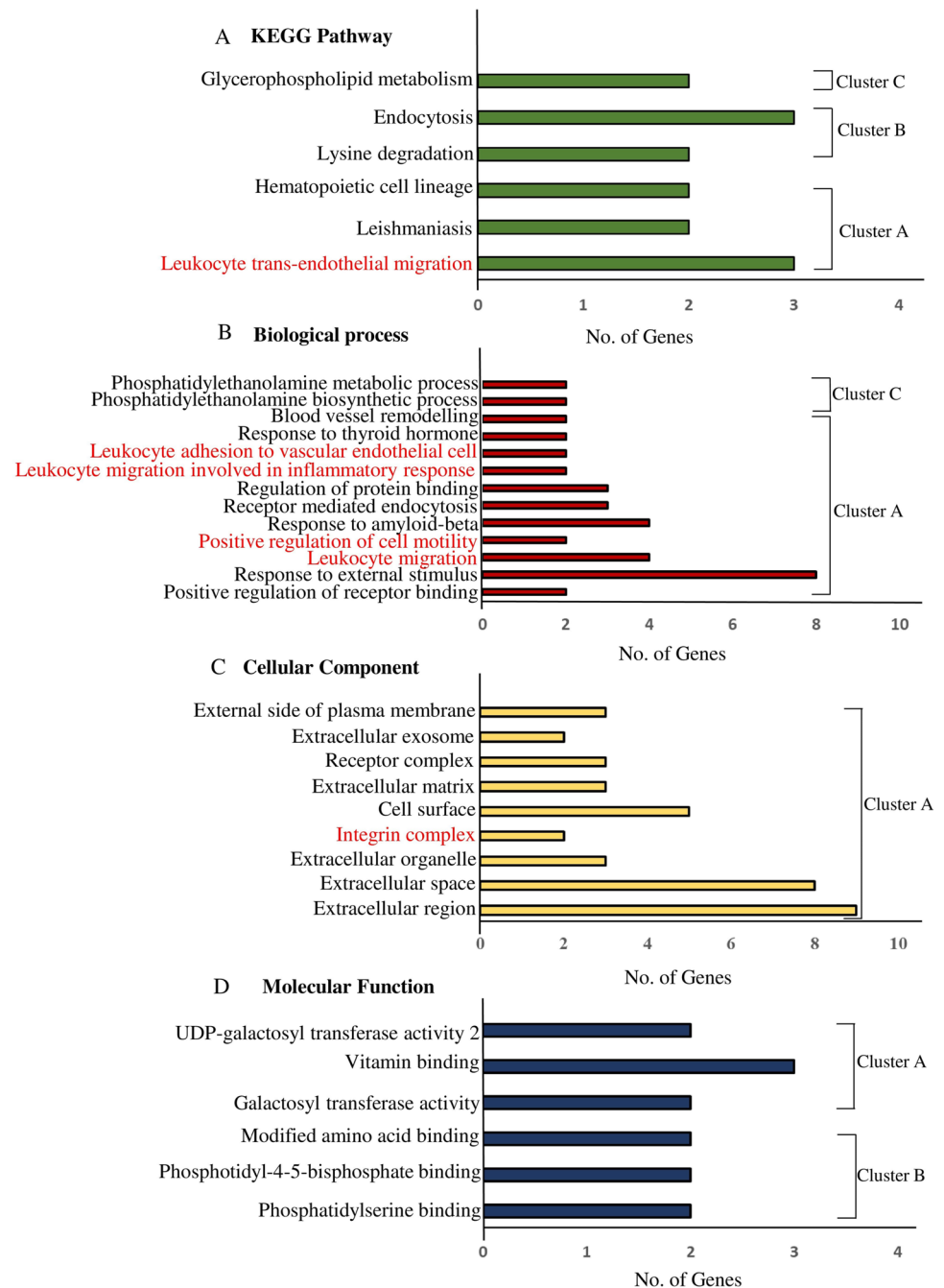


**Fig. 10** Transcriptomics characterisation of circulating leukocytes induced by L-ascorbic acid and  $\alpha$ -tocopherol supplementation under arsenic-exposed condition. Heatmap of 67 genes that were differentially expressed within leukocytes from each group (A). Volcano plot

of 67 genes of group I vs II (B). Volcano plot of 67 genes of group II vs III (C). Clustering analysis of 67 genes (D); green, downregulated; red, upregulated

**Fig. 11** Kyoto Encyclopaedia of Genes and Genomes (KEGG) pathway analyses of 67 genes (A), GO term biological process (B), analysis of 67 genes

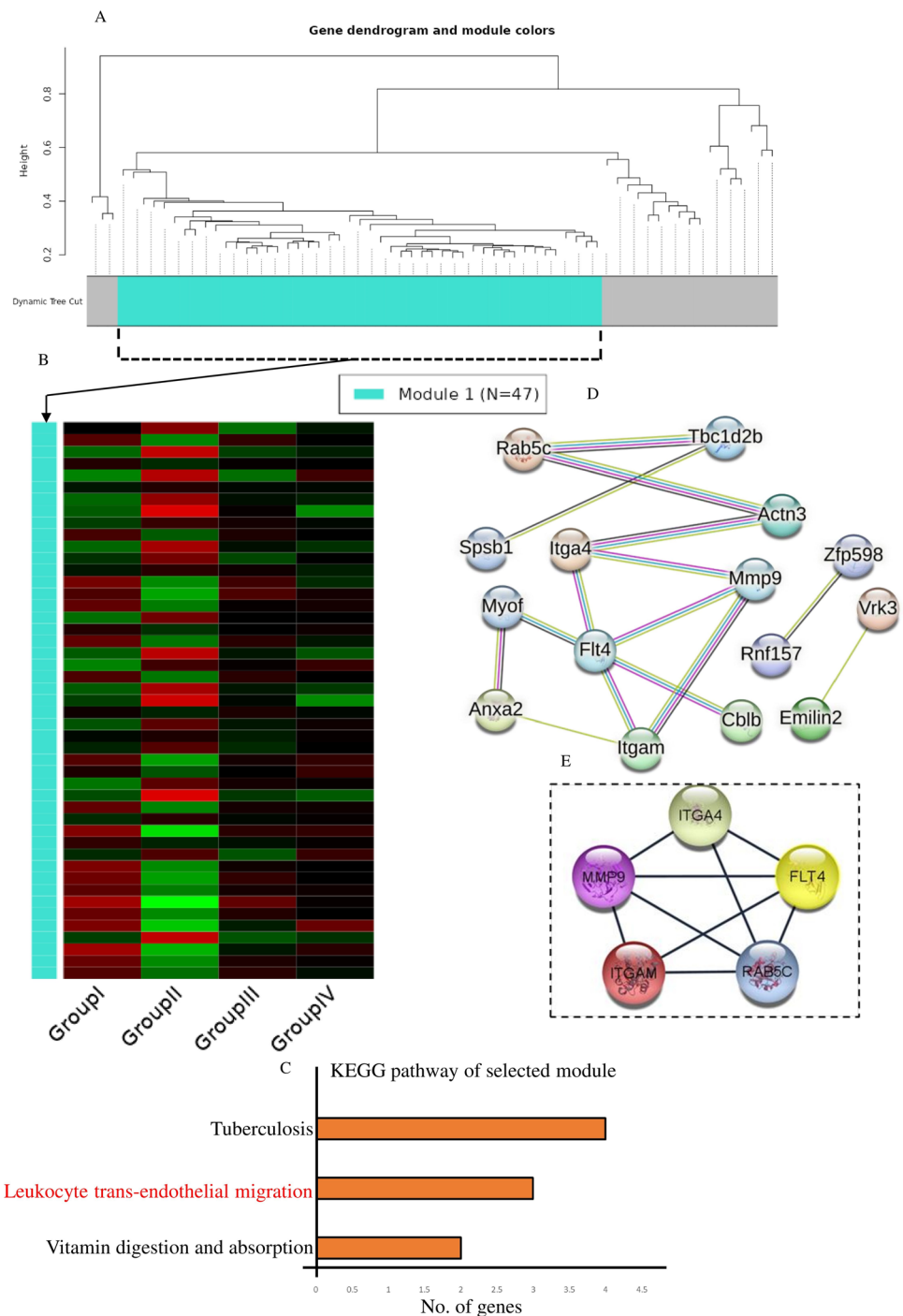


other studies showed that ascorbic acid enhanced the expression of hOGG1 (human 8-oxoguanine DNA N-glycosylase 1- DNA damage repair enzyme) [92] and XRCC1 — a gene involved in base excision repair [93]. Astley et al. demonstrated that there was a negative correlation in between plasma vitamin C and 8oxodG in PBMC DNA [94]. While tocopherol reduced DNA damage by influencing Dnmt1 (encodes an enzyme involved in transfer of the methyl group to cytosine of genomic DNA) and MLH 1 (encodes a crucial protein that involved in mismatch repair) gene expression [95]. Based on the aforesaid insights, it may be hypothesised

that L-AA and  $\alpha$ -T attenuated arsenic-mediated DNA damage of peripheral lymphocytes by influencing the DNA repairing enzymes.

Whole transcriptomics analysis revealed that arsenic exposure influenced trans-endothelial migration of lymphocytes by increasing the expression of Itgam, Itga4, and MMP-9 genes. It is well known that Itgam gene expresses integrin- $\alpha_M$  subunit, which form integrin- $\alpha_M\beta_2$  by heterodimerisation with integrin- $\beta_2$  subunit [96]. It has been shown that integrin- $\alpha_M\beta_2$  is expressed on the surface of polymorphonuclear monocytes, macrophages, natural killer cell,

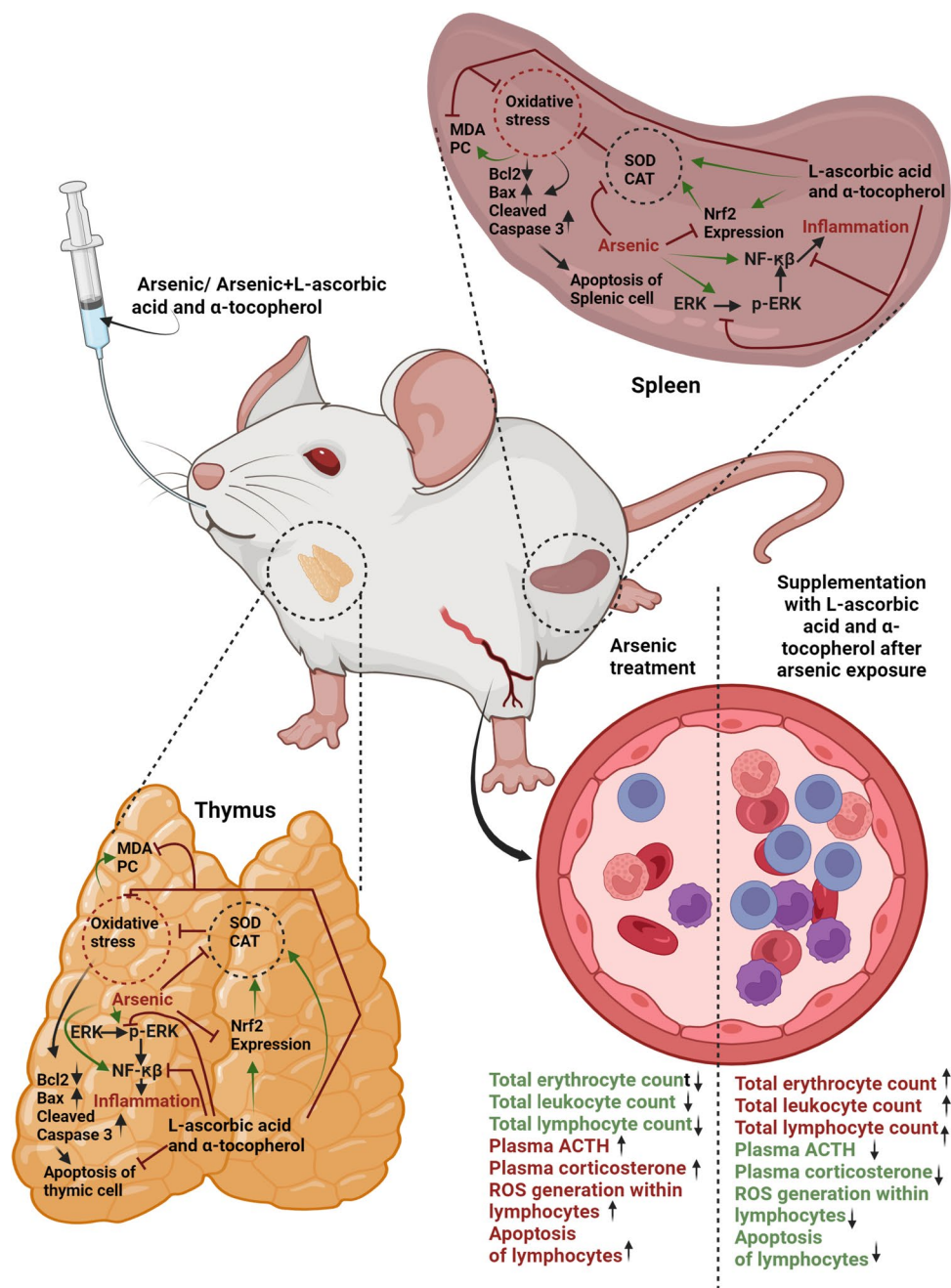
**Fig. 12** The weighted correlation network analysis (WGCNA) and Heatmap of genes of selected module (turquoise module) with a threshold of 0.75 (A, B); green, downregulated; red, upregulated. KEGG pathway of this turquoise module (C). Protein–protein interaction (PPI) network of screened 67 differentially expressed genes (DEGs) (D). cytoHubba analysis of PPI network in terms of degree centrality and shortest pathway (E)



some subpopulation of cytotoxic T cell, and involved in trans-endothelial migration of leukocytes [96, 97]. Itga4 gene expresses integrin- $\alpha_4$  subunit to form integrin- $\alpha_4\beta_1$  and also known as VLA-4 [98] which is involved in leukocyte migration along the vessel wall [99–101]. On the other hand, it was shown that MMP-9 plays a crucial role in leukocyte trans-endothelial migration [102, 103]. Therefore, it can be said that arsenic facilitated transient migration of leukocytes

through the endothelial cell layer by increasing the expression of Itgam, Itga4, and MMP-9 genes. Available data indicated that inflammation induced leukocyte trans-endothelial migration to the inflammation site which resulted in tissue injuries [104–110]. Lawson et al. showed that endotoxin-induced parenchymal cell apoptosis enhanced neutrophil infiltration and led to liver injury [111]. In 2000, Uchimura et al. reported that X-ray irradiation-induced apoptosis led to

**Fig. 13** Schematic diagram of the proposed hypothesis for the beneficial ability of supplementation of L-AA and  $\alpha$ -T in arsenic-induced immunotoxicities (created with BioRender.com)



neutrophil infiltration in the thymus [112]. In both in vivo and in vitro system, it was shown that neutrophil facilitated macrophage-mediated digestion of apoptotic cells [113]. Later, Kluger et al. showed that leukocyte-derived MMP-9 recruited proinflammatory macrophages in inflamed tissue [114]. Based on these insights, it can be hypothesised that arsenic-mediated oxidative stress-induced inflammation enhances trans-endothelial migration of leukocytes into affected tissues and causes tissue injuries, i.e., cellular-depleted areas in the thymus and expansion of the splenic

red-pulp areas. Furthermore, co-administration of L-AA and  $\alpha$ -T limited transient migration of leukocytes through the endothelial cell layer by decreasing the gene expression of *Itgam*, *Itga4*, and *MMP-9*. This study has certain limitations. Validation of RNA-sequencing data was not shown here. Leukocyte infiltration to the inflamed site was not shown here. Future research work is required to have a greater understanding of the molecular mechanisms related to arsenic-mediated leukocyte infiltration to the inflammatory site and its amelioration by L-AA and  $\alpha$ -T co-administration.



## Conclusion

In summary, our data showed that supplementation of L-AA and  $\alpha$ -T mitigates arsenic-induced immunotoxicities. These positive benefits were found to be directly related to its capacity to upregulate the expression of Nrf2 which subsequently restores SOD and CAT activities and inhibit arsenic-mediated oxidative stress-induced inflammation and apoptosis (Fig. 13).

Until now, there is no direct evidence regarding the arsenic-mediated increased plasma corticosterone-induced apoptosis of thymocytes and splenocytes. In the present study, we have measured the plasma ACTH and corticosterone levels along with quantification of total thymocyte and splenocyte count to establish the fact that arsenic disrupts the negative feedback mechanism of the HPA axis which in turn leads to apoptosis of thymocyte and splenocyte. The present study shows the positive impact of L-AA and  $\alpha$ -T co-administration in prevention of thymocyte and splenocyte reduction by restoring the plasma ACTH and corticosterone level towards normal.

Moreover, our study is the first to report that co-administration of L-AA and  $\alpha$ -T mitigates the arsenic-mediated inflammation by lowering the phosphorylation level of ERK-1/2 and expression of NF- $\kappa$ B within the thymus and spleen of Wistar rats. Furthermore, we are the first to show that arsenic increases the expression of MMP9, Itga4, and Itgam which is involved in transient migration of leukocytes through the endothelial cell layer. On the other hand, leukocyte trans-endothelial migration is limited by L-AA and  $\alpha$ -T co-administration by keeping Itgam, Itga4, and MMP9 gene expression at a lower level.

**Author Contribution** Jeet Maity: conceptualisation, data curation, analysis, investigation, validation, writing — original draft. Priyanka Pal: data curation. Prabir Kumar Mukhopadhyay and Ranjana Pal: conceptualisation, funding acquisition, project administration, resources, validation.

**Funding** This work was supported by a grant from the research programme (No: 5/8–4/17/Env/2020-NCD-II) funded by the Indian Council of Medical Research (ICMR), Department of Health Research, Ministry of Health and Family welfare, Government of India (New Delhi, India). We are also grateful to DST-FIST, Government of India (DLS[SR/FST/LSI-560/2013(C)]) and DBT-BUILDER (BT/INF/22/SP45088/2022).

**Data Availability** The data that supports the finding of the study are available from the corresponding author upon reasonable request.

## Declarations

**Ethical Consent from Institutional Animal Ethical Committee** Prior to the start of the animal experiment, the Institutional Animal Ethics Committee provided its formal consent (Sanction No. PU/IAEC/PM/24).

**Competing interests** The authors declare no competing interests.

**Conflict of Interest** The authors declare no competing interests.

## References

- Duan X, Gao S, Li J et al (2017) Acute arsenic exposure induces inflammatory responses and CD4+ T cell subpopulations differentiation in spleen and thymus with the involvement of MAPK, NF- $\kappa$ B, and Nrf2. *Mol Immunol* 81:160–172. <https://doi.org/10.1016/j.molimm.2016.12.005>
- Nicomel N, Leus K, Folens K et al (2015) Technologies for arsenic removal from water: current status and future perspectives. *Int J Environ Res Public Health* 13:62. <https://doi.org/10.3390/ijerph13010062>
- Islam K, Wang QQ, Naranmandura H (2015) Molecular mechanisms of arsenic toxicity. *Advances in Molecular Toxicology* 9: 77–107. <https://doi.org/10.1016/B978-0-12-802229-0.00002-5>
- Buchet JP, Lauwerys R, Roels H (1981) Comparison of the urinary excretion of arsenic metabolites after a single oral dose of sodium arsenite, monomethylarsonate, or dimethylarsinate in man. *Int Arch Occup Environ Health* 48:71–79. <https://doi.org/10.1007/BF00405933>
- Lin K, Lu S, Wang J, Yang Y (2015) The arsenic contamination of rice in Guangdong Province, the most economically dynamic provinces of China: arsenic speciation and its potential health risk. *Environ Geochem Health* 37:353–361. <https://doi.org/10.1007/s10653-014-9652-1>
- Babar MM, Tariq A (2018) Status of arsenic toxicity in the world. In: *Mechanisms of arsenic toxicity and tolerance in plants*. Springer, Singapore. 11:457–481. [https://doi.org/10.1007/978-981-13-1292-2\\_18](https://doi.org/10.1007/978-981-13-1292-2_18)
- Hamad SH, Schauer JJ, Shafer MM et al (2014) Risk assessment of total and bioavailable potentially toxic elements (PTEs) in urban soils of Baghdad-Iraq. *Sci Total Environ* 494–495:39–48. <https://doi.org/10.1016/j.scitotenv.2014.06.006>
- Weindorf DC, Paulette L, Man T (2013) In-situ assessment of metal contamination via portable X-ray fluorescence spectroscopy: Zlatna, Romania. *Environ Pollut* 182:92–100. <https://doi.org/10.1016/j.envpol.2013.07.008>
- Varsányi I, Kovács LÓ (2006) Arsenic, iron and organic matter in sediments and groundwater in the Pannonian Basin, Hungary. *Appl Geochemistry* 21:949–963. <https://doi.org/10.1016/j.apgeochem.2006.03.006>
- Acharyya SK, Lahiri S, Raymahashay BC, Bhowmik A (2000) Arsenic toxicity of groundwater in parts of the Bengal basin in India and Bangladesh: the role of Quaternary stratigraphy and Holocene sea-level fluctuation. *Environ Geol* 39:1127–1137. <https://doi.org/10.1007/s002540000107>
- Shaji E, Santosh M, Sarath KV et al (2021) Arsenic contamination of groundwater: a global synopsis with focus on the Indian Peninsula. *Geosci Front* 12:101079. <https://doi.org/10.1016/j.gsf.2020.08.015>
- Niedzwiecki MM, Liu X, Zhu H et al (2018) Serum homocysteine, arsenic methylation, and arsenic-induced skin lesion incidence in Bangladesh: a one-carbon metabolism candidate gene study. *Environ Int* 113:133–142. <https://doi.org/10.1016/j.envint.2018.01.015>
- Kuo C-C, Moon KA, Wang S-L et al (2017) The association of arsenic metabolism with cancer, cardiovascular disease, and diabetes: a systematic review of the epidemiological evidence.

- Environ Health Perspect 125:087001. <https://doi.org/10.1289/EHP577>
14. Mohammed Abdul KS, Jayasinghe SS, Chandana EPS et al (2015) Arsenic and human health effects: a review. *Environ Toxicol Pharmacol* 40:828–846. <https://doi.org/10.1016/j.etap.2015.09.016>
  15. Leonardi G, Vahter M, Clemens F et al (2012) Inorganic arsenic and basal cell carcinoma in areas of Hungary, Romania, and Slovakia: a case–control study. *Environ Health Perspect* 120:721–726. <https://doi.org/10.1289/ehp.1103534>
  16. Kumar A, Ali M, Kumar R et al (2021) Arsenic exposure in Indo Gangetic plains of Bihar causing increased cancer risk. *Sci Rep* 11:2376. <https://doi.org/10.1038/s41598-021-81579-9>
  17. Gera R, Singh V, Mitra S et al (2017) Arsenic exposure impels CD4 commitment in thymus and suppress T cell cytokine secretion by increasing regulatory T cells. *Sci Rep* 7:7140. <https://doi.org/10.1038/s41598-017-07271-z>
  18. Rahman HH, Niemann D, Singh D (2020) Arsenic exposure and association with hepatitis E IgG antibodies. *Occup Dis Environ Med* 08:111–122. <https://doi.org/10.4236/odem.2020.83009>
  19. Raqib R, Ahmed S, Sultana R et al (2009) Effects of in utero arsenic exposure on child immunity and morbidity in rural Bangladesh. *Toxicol Lett* 185:197–202. <https://doi.org/10.1016/j.toxlet.2009.01.001>
  20. Andrew AS, Jewell DA, Mason RA et al (2008) Drinking-water arsenic exposure modulates gene expression in human lymphocytes from a U.S. population. *Environ Health Perspect* 116:524–531. <https://doi.org/10.1289/ehp.10861>
  21. Moore S, Prentice A, Wagatsuma Y et al (2009) Early-life nutritional and environmental determinants of thymic size in infants born in rural Bangladesh. *Acta Paediatr* 98:1168–1175. <https://doi.org/10.1111/j.1651-2227.2009.01292.x>
  22. Xu H, McClain S, Medina S et al (2016) Differential sensitivities of bone marrow, spleen and thymus to genotoxicity induced by environmentally relevant concentrations of arsenite. *Toxicol Lett* 262:55–61. <https://doi.org/10.1016/j.toxlet.2016.09.008>
  23. Jamal Z, Das J, Ghosh S et al (2020) Arsenic-induced immunomodulatory effects disorient the survival-death interface by stabilizing the Hsp90/Beclin1 interaction. *Chemosphere* 238:124647. <https://doi.org/10.1016/j.chemosphere.2019.124647>
  24. Chen F, Luo Y, Li C et al (2021) Sub-chronic low-dose arsenic in rice exposure induces gut microbiome perturbations in mice. *Ecotoxicol Environ Saf* 227:112934. <https://doi.org/10.1016/j.ecoenv.2021.112934>
  25. Soto-Peña GA, Luna AL, Acosta-Saavedra L et al (2006) Assessment of lymphocyte subpopulations and cytokine secretion in children exposed to arsenic. *FASEB J* 20:779–781. <https://doi.org/10.1096/fj.05-4860fje>
  26. Biswas R, Ghosh P, Banerjee N et al (2008) Analysis of T-cell proliferation and cytokine secretion in the individuals exposed to arsenic. *Hum Exp Toxicol* 27:381–386. <https://doi.org/10.1177/0960327108094607>
  27. Yan N, Xu G, Zhang C et al (2020) Chronic arsenic exposure induces the time-dependent modulation of inflammation and immunosuppression in spleen. *Cell Biosci* 10:91. <https://doi.org/10.1186/s13578-020-00448-6>
  28. Delgado J, Dufour L, Grimaldo J et al (2000) Effects of arsenite on central monoamines and plasmatic levels of adrenocorticotrophic hormone (ACTH) in mice. *Toxicol Lett* 117:61–67. [https://doi.org/10.1016/S0378-4274\(00\)00240-X](https://doi.org/10.1016/S0378-4274(00)00240-X)
  29. Goggin SL, Labrecque MT, Allan AM (2012) Perinatal exposure to 50 ppb sodium arsenate induces hypothalamic-pituitary-adrenal axis dysregulation in male C57BL/6 mice. *Neurotoxicology* 33:1338–1345. <https://doi.org/10.1016/j.neuro.2012.08.010>
  30. Barone KS, O'Brien PCM, Stevenson JR (1993) Characterization and mechanisms of thymic atrophy in protein-malnourished mice: role of corticosterone. *Cell Immunol* 148:226–233. <https://doi.org/10.1006/cimm.1993.1105>
  31. Matsuoka K, Tsuji D, Taki T, Itoh K (2011) Thymic involution and corticosterone level in Sandhoff disease model mice: new aspects the pathogenesis of GM2 gangliosidosis. *J Inher Metab Dis* 34:1061–1068. <https://doi.org/10.1007/s10545-011-9316-6>
  32. Hernandez ME, Martinez-Mota L, Salinas C et al (2013) Chronic stress induces structural alterations in splenic lymphoid tissue that are associated with changes in corticosterone levels in Wistar-Kyoto rats. *Biomed Res Int* 2013:1–6. <https://doi.org/10.1155/2013/868742>
  33. Biswas P, Mukhopadhyay A, Kabir SN, Mukhopadhyay PK (2019) High-protein diet ameliorates arsenic-induced oxidative stress and antagonizes uterine apoptosis in rats. *Biol Trace Elem Res* 192:222–233. <https://doi.org/10.1007/s12011-019-1657-2>
  34. Flora SJS, Mittal M, Mehta A (2008) Heavy metal induced oxidative stress & its possible reversal by chelation therapy. *Indian J Med Res* 128:501–523
  35. Pal P, De A, Roychowdhury T, Mukhopadhyay PK (2022) Vitamin C and E supplementation can ameliorate NaF mediated testicular and spermatozoal DNA damages in adult Wistar rats. *Biomarkers* 27:361–374. <https://doi.org/10.1080/1354750X.2022.2048891>
  36. Hamdan DI, Tawfeek N, El-Shiekh RA et al (2022) Salix subserata bark extract-loaded chitosan nanoparticles attenuate neurotoxicity induced by sodium arsenate in rats in relation with HPLC–PDA–ESI–MS/MS profile. *AAPS PharmSciTech* 24:15. <https://doi.org/10.1208/s12249-022-02478-4>
  37. Sankar P, Gopal Telang A, Kalaiavanan R et al (2015) Effects of nanoparticle-encapsulated curcumin on arsenic-induced liver toxicity in rats. *Environ Toxicol* 30:628–637. <https://doi.org/10.1002/tox.21940>
  38. Organisation for Economic Co-operation and Development (2008) Test No. 407: repeated dose 28-day oral toxicity study in rodents. OECD Guidelines for the Testing of Chemicals, Section 4, OECD Publishing, Paris. <https://doi.org/10.1787/9789264070684>
  39. Chandravanshi LP, Patel DK (2017) Subchronic early life arsenic exposure at low doses impaired the biogenic amine neurotransmitter and nitric oxide levels in different brain regions of rats. *J Environ Anal Toxicol* 07: <https://doi.org/10.4172/2161-0525.1000477>
  40. Baran-Gale J, Morgan MD, Maio S et al (2020) Ageing compromises mouse thymus function and remodels epithelial cell differentiation. *Elife* 9: <https://doi.org/10.7554/eLife.56221>
  41. Ghosh C, Bishay B (2015) Characterization of Toll-like receptor-4 (TLR-4) in the spleen and thymus of Swiss albino mice and its modulation in experimental endotoxemia. *J Immunol Res* 2015:1–13. <https://doi.org/10.1155/2015/137981>
  42. Martin JP, Dailey M, Sugarman E (1987) Negative and positive assays of superoxide dismutase based on hematoxylin autooxidation. *Arch Biochem Biophys* 255:329–336. [https://doi.org/10.1016/0003-9861\(87\)90400-0](https://doi.org/10.1016/0003-9861(87)90400-0)
  43. Claiborne, A. (1985). Catalase activity. In: Greenwald, R.A. (ed.) *Handbook of methods of oxygen radical research*. CRC Press, Boca Raton, Florida, p 283–284
  44. Levine RL, Williams JA, Stadtman EP, Shacter E (1994) Carbonyl assays for determination of oxidatively modified proteins. 233:346–357. [https://doi.org/10.1016/S0076-6879\(94\)33040-9](https://doi.org/10.1016/S0076-6879(94)33040-9)
  45. Brown-Borg H, Johnson WT, Rakoczy S, Romanick M (2001) Mitochondrial oxidant generation and oxidative damage in Ames

- dwarf and GH transgenic mice. *Age (Omaha)* 24:85–96. <https://doi.org/10.1007/s11357-001-0012-6>
46. Khanam R, Sengupta A, Mukhopadhyay D, Chakraborty S (2022) Identification of Adamts4 as a novel adult cardiac injury biomarker with therapeutic implications in patients with cardiac injuries. *Sci Rep* 12:9898. <https://doi.org/10.1038/s41598-022-13918-3>
  47. Killick KE, Browne JA, DE Park S et al (2011) Genome-wide transcriptional profiling of peripheral blood leukocytes from cattle infected with *Mycobacterium bovis* reveals suppression of host immune genes. *BMC Genomics* 12:611. <https://doi.org/10.1186/1471-2164-12-611>
  48. Gong T, Wang C-F, Yuan J-R et al (2015) Inhibition of tumor growth and immunomodulatory effects of flavonoids and scutebarbatines of *Scutellaria barbata* D. Don in Lewis-bearing C57BL/6 mice. *Evid Based Complement Alternat Med* 2015:630760. <https://doi.org/10.1155/2015/630760>
  49. Kile ML, Houseman EA, Baccarelli AA et al (2014) Effect of prenatal arsenic exposure on DNA methylation and leukocyte subpopulations in cord blood. *Epigenetics* 9:774–782. <https://doi.org/10.4161/epi.28153>
  50. Burns LA, Munson AE (1993) Gallium arsenide selectively inhibits T cell proliferation and alters expression of CD25 (IL-2R/p55). *J Pharmacol Exp Ther* 265:178–186
  51. Burchiel SW, Lauer FT, Factor-Litvak P et al (2020) Arsenic exposure associated T cell proliferation, smoking, and vitamin D in Bangladeshi men and women. *PLoS One* 15:e0234965. <https://doi.org/10.1371/journal.pone.0234965>
  52. Akter R, Neelotpol S, Kabir MT (2022) Effect of *Allium sativum* methanol extract in amelioration of arsenic-induced toxicity in Swiss albino mice. *Phytomedicine Plus* 2:100192. <https://doi.org/10.1016/j.phyplu.2021.100192>
  53. Ozerkan D, Ozsoy N, Cebesoy S (2014) Response of thymus lymphocytes to streptozotocin-induced diabetes and exogenous vitamin C administration in rats. *Microscopy* 63:409–417. <https://doi.org/10.1093/jmicro/dfu029>
  54. Kim H, Bae S, Yu Y et al (2012) The analysis of vitamin C concentration in organs of gulo -/- mice upon vitamin C withdrawal. *Immune Netw* 12:18. <https://doi.org/10.4110/in.2012.12.1.18>
  55. Moriguchi S (1998) The role of vitamin E in T-cell differentiation and the decrease of cellular immunity with aging. *BioFactors* 7:77–86. <https://doi.org/10.1002/biof.5520070111>
  56. Herman JP, Cullinan WE, Young EA et al (1992) Selective fore-brain fiber tract lesions implicate ventral hippocampal structures in tonic regulation of paraventricular nucleus corticotropin-releasing hormone (CRH) and arginine vasopressin (AVP) mRNA expression. *Brain Res* 592:228–238. [https://doi.org/10.1016/0006-8993\(92\)91680-D](https://doi.org/10.1016/0006-8993(92)91680-D)
  57. Löwenberg M, Verhaar AP, Bilderbeek J et al (2006) Glucocorticoids cause rapid dissociation of a T-cell-receptor-associated protein complex containing LCK and FYN. *EMBO Rep* 7:1023–1029. <https://doi.org/10.1038/sj.embor.7400775>
  58. Löwenberg M, Tuynman J, Bilderbeek J et al (2005) Rapid immunosuppressive effects of glucocorticoids mediated through Lck and Fyn. *Blood* 106:1703–1710. <https://doi.org/10.1182/blood-2004-12-4790>
  59. Baschant U, Tuckermann J (2010) The role of the glucocorticoid receptor in inflammation and immunity. *J Steroid Biochem Mol Biol* 120:69–75. <https://doi.org/10.1016/j.jsbmb.2010.03.058>
  60. Zhang N, Zhao W, Hu Z-J et al (2021) Protective effects and mechanisms of high-dose vitamin C on sepsis-associated cognitive impairment in rats. *Sci Rep* 11:14511. <https://doi.org/10.1038/s41598-021-93861-x>
  61. Tveden-Nyborg P, Johansen LK, Raida Z et al (2009) Vitamin C deficiency in early postnatal life impairs spatial memory and reduces the number of hippocampal neurons in guinea pigs. *Am J Clin Nutr* 90:540–546. <https://doi.org/10.3945/ajcn.2009.27954>
  62. Chang B-J, Jang B-J, Son TG et al (2012) Ascorbic acid ameliorates oxidative damage induced by maternal low-level lead exposure in the hippocampus of rat pups during gestation and lactation. *Food Chem Toxicol* 50:104–108. <https://doi.org/10.1016/j.fct.2011.09.043>
  63. Gurer H, Ercal N (2000) Can antioxidants be beneficial in the treatment of lead poisoning? *Free Radic Biol Med* 29:927–945. [https://doi.org/10.1016/S0891-5849\(00\)00413-5](https://doi.org/10.1016/S0891-5849(00)00413-5)
  64. Tomé AR, Feng D, Freitas RM (2010) The effects of alpha-tocopherol on hippocampal oxidative stress prior to in pilocarpine-induced seizures. *Neurochem Res* 35:580–587. <https://doi.org/10.1007/s11064-009-0102-x>
  65. Nesari A, Mansouri MT, Khodayar MJ, Rezaei M (2021) Preadministration of high-dose alpha-tocopherol improved memory impairment and mitochondrial dysfunction induced by proteasome inhibition in rat hippocampus. *Nutr Neurosci* 24:119–129. <https://doi.org/10.1080/1028415X.2019.1601888>
  66. Mahmoud KZ, Edens FW, Eisen EJ, Havenstein GB (2004) Ascorbic acid decreases heat shock protein 70 and plasma corticosterone response in broilers (*Gallus gallus domesticus*) subjected to cyclic heat stress. *Comp Biochem Physiol Part B Biochem Mol Biol* 137:35–42. <https://doi.org/10.1016/j.cbpc.2003.09.013>
  67. Ibrahim IAA, Kamisah Y, Nafeeza MI, Azlina MFN (2012) The effects of palm vitamin E on stress hormone levels and gastric lesions in stress-induced rats. *Arch Med Sci* 1:22–29. <https://doi.org/10.5114/aoms.2012.27276>
  68. Janasik B, Reszka E, Stanislawski M et al (2018) Effect of arsenic exposure on NRF2-KEAP1 pathway and epigenetic modification. *Biol Trace Elem Res* 185:11–19. <https://doi.org/10.1007/s12011-017-1219-4>
  69. Jin W, Xue Y, Xue Y et al (2020) Tannic acid ameliorates arsenic trioxide-induced nephrotoxicity, contribution of NF- $\kappa$ B and Nrf2 pathways. *Biomed Pharmacother* 126:110047. <https://doi.org/10.1016/j.biopha.2020.110047>
  70. Khadrawy O, Gebremedhn S, Salilew-Wondim D et al (2019) Endogenous and exogenous modulation of Nrf2 mediated oxidative stress response in bovine granulosa cells: potential implication for ovarian function. *Int J Mol Sci* 20:1635. <https://doi.org/10.3390/ijms20071635>
  71. Khan MM, Kim YK, Bilkis T et al (2020) Reduction of oxidative stress through activating the Nrf2 mediated HO-1 antioxidant efficacy signaling pathway by MS15, an antimicrobial peptide from *Bacillus velezensis*. *Antioxidants* 9:934. <https://doi.org/10.3390/antiox9100934>
  72. Xu L-L, Zhao B, Sun S-L et al (2020) High-dose vitamin C alleviates pancreatic injury via the NRF2/NQO1/HO-1 pathway in a rat model of severe acute pancreatitis. *Ann Transl Med* 8:852–852. <https://doi.org/10.21037/atm-19-4552>
  73. Feng Z, Liu Z, Li X et al (2010)  $\alpha$ -Tocopherol is an effective phase II enzyme inducer: protective effects on acrolein-induced oxidative stress and mitochondrial dysfunction in human retinal pigment epithelial cells. *J Nutr Biochem* 21:1222–1231. <https://doi.org/10.1016/j.jnutbio.2009.10.010>
  74. Vineetha RC, Binu P, Arathi P, Nair RH (2018) L-ascorbic acid and  $\alpha$ -tocopherol attenuate arsenic trioxide-induced toxicity in H9c2 cardiomyocytes by the activation of Nrf2 and Bcl2 transcription factors. *Toxicol Mech Methods* 28:353–360. <https://doi.org/10.1080/15376516.2017.1422578>
  75. Rui W, Guan L, Zhang F et al (2016) PM 2.5 -induced oxidative stress increases adhesion molecules expression in human endothelial cells through the ERK/AKT/NF- $\kappa$ B-dependent pathway. *J Appl Toxicol* 36:48–59. <https://doi.org/10.1002/jat.3143>

76. Bodaghi-Namileh V, Sepand MR, Omid A et al (2018) Acetyl-L-carnitine attenuates arsenic-induced liver injury by abrogation of mitochondrial dysfunction, inflammation, and apoptosis in rats. *Environ Toxicol Pharmacol* 58:11–20. <https://doi.org/10.1016/j.etap.2017.12.005>
77. Fry RC, Navasumrit P, Valiathan C et al (2007) Activation of inflammation/NF- $\kappa$ B signaling in infants born to arsenic-exposed mothers. *PLoS Genet* 3:e207. <https://doi.org/10.1371/journal.pgen.0030207>
78. Aguilera O, Muñoz-Sagastibelza M, Torrejón B et al (2016) Vitamin C uncouples the Warburg metabolic switch in KRAS mutant colon cancer. *Oncotarget* 7:47954–47965. <https://doi.org/10.18632/oncotarget.10087>
79. Redza-Dutordoir M, Averill-Bates DA (2016) Activation of apoptosis signalling pathways by reactive oxygen species. *Biochim Biophys Acta - Mol Cell Res* 1863:2977–2992. <https://doi.org/10.1016/j.bbamer.2016.09.012>
80. Tzifi F, Economopoulou C, Gourgiotis D et al (2012) The role of BCL2 family of apoptosis regulator proteins in acute and chronic leukemias. *Adv Hematol* 2012:1–15. <https://doi.org/10.1155/2012/524308>
81. Xia Y, Hao G, Yang Y (2009) Study on reproductive and immune toxicity of male rats exposed to As<sub>2</sub>O<sub>3</sub>. *Wei Sheng Yan Jiu* 38:720–722
82. Rousselot P, Larghero J, Labaume S et al (2004) Arsenic trioxide is effective in the treatment of multiple myeloma in SCID mice. *Eur J Haematol* 72:166–171. <https://doi.org/10.1046/j.0902-4441.2003.00194.x>
83. Burchiel SW, Lauer FT, Beswick EJ et al (2014) Differential susceptibility of human peripheral blood T cells to suppression by environmental levels of sodium arsenite and monomethylarsonous acid. *PLoS One* 9:e109192. <https://doi.org/10.1371/journal.pone.0109192>
84. Grollman AP, Moriya M (1993) Mutagenesis by 8-oxoguanine: an enemy within. *Trends Genet* 9:246–249. [https://doi.org/10.1016/0168-9525\(93\)90089-Z](https://doi.org/10.1016/0168-9525(93)90089-Z)
85. Shockley AH, Doo DW, Rodriguez GP, Crouse GF (2013) Oxidative damage and mutagenesis in *Saccharomyces cerevisiae*: genetic studies of pathways affecting replication fidelity of 8-oxoguanine. *Genetics* 195:359–367. <https://doi.org/10.1534/genetics.113.153874>
86. Ba X, Boldogh I (2018) 8-Oxoguanine DNA glycosylase 1: beyond repair of the oxidatively modified base lesions. *Redox Biol* 14:669–678. <https://doi.org/10.1016/j.redox.2017.11.008>
87. Ebert F, Weiss A, Bülttemeyer M et al (2011) Arsenicals affect base excision repair by several mechanisms. *Mutat Res Mol Mech Mutagen* 715:32–41. <https://doi.org/10.1016/j.mrfmmm.2011.07.004>
88. Sykora P, Snow ET (2008) Modulation of DNA polymerase beta-dependent base excision repair in cultured human cells after low dose exposure to arsenite. *Toxicol Appl Pharmacol* 228:385–394. <https://doi.org/10.1016/j.taap.2007.12.019>
89. Idriss HT, Al-Assar O, Wilson SH (2002) DNA polymerase  $\beta$ . *Int J Biochem Cell Biol* 34:321–324. [https://doi.org/10.1016/S1357-2725\(01\)00131-5](https://doi.org/10.1016/S1357-2725(01)00131-5)
90. Andrew AS, Karagas MR, Hamilton JW (2003) Decreased DNA repair gene expression among individuals exposed to arsenic in United States drinking water. *Int J Cancer* 104:263–268. <https://doi.org/10.1002/ijc.10968>
91. Kadirvel R, Sundaram K, Mani S et al (2007) Supplementation of ascorbic acid and  $\alpha$ -tocopherol prevents arsenic-induced protein oxidation and DNA damage induced by arsenic in rats. *Hum Exp Toxicol* 26:939–946. <https://doi.org/10.1177/0960327107087909>
92. Tarng D-C, Liu T-Y, Huang T-P (2004) Protective effect of vitamin C on 8-hydroxy-2'-deoxyguanosine level in peripheral blood lymphocytes of chronic hemodialysis patients. *Kidney Int* 66:820–831. <https://doi.org/10.1111/j.1523-1755.2004.00809.x>
93. Rossner P, Uhlirva K, Beskid O et al (2011) Expression of XRCC5 in peripheral blood lymphocytes is upregulated in subjects from a heavily polluted region in the Czech Republic. *Mutat Res Mol Mech Mutagen* 713:76–82. <https://doi.org/10.1016/j.mrfmmm.2011.06.001>
94. Astley SB, Elliott RM, Archer DB, Southon S (2004) Evidence that dietary supplementation with carotenoids and carotenoid-rich foods modulates the DNA damage:repair balance in human lymphocytes. *Br J Nutr* 91:63–72. <https://doi.org/10.1079/BJN20031001>
95. Remely M, Ferk F, Sterneder S et al (2017) Vitamin E modifies high-fat diet-induced increase of DNA strand breaks, and changes in expression and DNA methylation of Dnmt1 and MLH1 in C57BL/6J male mice. *Nutrients* 9:607. <https://doi.org/10.3390/nu9060607>
96. Solovjov DA, Pluskota E, Plow EF (2005) Distinct roles for the  $\alpha$  and  $\beta$  subunits in the functions of integrin  $\alpha$ M $\beta$ 2. *J Biol Chem* 280:1336–1345. <https://doi.org/10.1074/jbc.M406968200>
97. Jawhara S, Pluskota E, Cao W et al (2017) Distinct effects of integrins  $\alpha$ X $\beta$ 2 and  $\alpha$ M $\beta$ 2 on leukocyte subpopulations during inflammation and antimicrobial responses. *Infect Immun* 85:. <https://doi.org/10.1128/IAI.00644-16>
98. Schaefer A, Hordijk PL (2015) Cell-stiffness-induced mechanosignaling – a key driver of leukocyte transendothelial migration. *J Cell Sci* 128:2221–2230. <https://doi.org/10.1242/jcs.163055>
99. Gerhardt T, Ley K (2015) Monocyte trafficking across the vessel wall. *Cardiovasc Res* 107:321–330. <https://doi.org/10.1093/cvr/cvv147>
100. Weninger W, Biro M, Jain R (2014) Leukocyte migration in the interstitial space of non-lymphoid organs. *Nat Rev Immunol* 14:232–246. <https://doi.org/10.1038/nri3641>
101. Schwartz AB, Campos OA, Criado-Hidalgo E et al (2021) Elucidating the biomechanics of leukocyte transendothelial migration by quantitative imaging. *Front Cell Dev Biol* 9:. <https://doi.org/10.3389/fcell.2021.635263>
102. Lindner JR, Kahn ML, Coughlin SR et al (2000) Delayed onset of inflammation in protease-activated receptor-2-deficient mice. *J Immunol* 165:6504–6510. <https://doi.org/10.4049/jimmunol.165.11.6504>
103. Khandoga A, Kessler JS, Hanschen M et al (2006) Matrix metalloproteinase-9 promotes neutrophil and T cell recruitment and migration in the postschemic liver. *J Leukoc Biol* 79:1295–1305. <https://doi.org/10.1189/jlb.0805468>
104. Kroon J, Schaefer A, van Rijssel J et al (2018) Inflammation-sensitive myosin-X functionally supports leukocyte extravasation by Cdc42-mediated ICAM-1-rich endothelial filopodia formation. *J Immunol* 200:1790–1801. <https://doi.org/10.4049/jimmunol.1700702>
105. de Oliveira S, Rosowski EE, Huttenlocher A (2016) Neutrophil migration in infection and wound repair: going forward in reverse. *Nat Rev Immunol* 16:378–391. <https://doi.org/10.1038/nri.2016.49>
106. Cantin AM, Hartl D, Konstan MW, Chmiel JF (2015) Inflammation in cystic fibrosis lung disease: pathogenesis and therapy. *J Cyst Fibros* 14:419–430. <https://doi.org/10.1016/j.jcf.2015.03.003>
107. Wright HL, Moots RJ, Edwards SW (2014) The multifactorial role of neutrophils in rheumatoid arthritis. *Nat Rev Rheumatol* 10:593–601. <https://doi.org/10.1038/nrrheum.2014.80>
108. Tsukamoto T, Chanthaphavong RS, Pape H-C (2010) Current theories on the pathophysiology of multiple organ failure after

- trauma. *Injury* 41:21–26. <https://doi.org/10.1016/j.injury.2009.07.010>
109. Ley K, Laudanna C, Cybulsky MI, Nourshargh S (2007) Getting to the site of inflammation: the leukocyte adhesion cascade updated. *Nat Rev Immunol* 7:678–689. <https://doi.org/10.1038/nri2156>
110. Luster AD, Alon R, von Andrian UH (2005) Immune cell migration in inflammation: present and future therapeutic targets. *Nat Immunol* 6:1182–1190. <https://doi.org/10.1038/ni1275>
111. Lawson JA, Fisher MA, Simmons CA et al (1998) Parenchymal cell apoptosis as a signal for sinusoidal sequestration and transendothelial migration of neutrophils in murine models of endotoxin and fas-antibody-induced liver injury. *Hepatology* 28:761–767. <https://doi.org/10.1002/hep.510280324>
112. Uchimura E, Watanabe N, Niwa O et al (2000) Transient infiltration of neutrophils into the thymus in association with apoptosis induced by whole-body X-irradiation. *J Leukoc Biol* 67:780–784. <https://doi.org/10.1002/jlb.67.6.780>
113. Iyoda T, Nagata K, Akashi M, Kobayashi Y (2005) Neutrophils accelerate macrophage-mediated digestion of apoptotic cells in vivo as well as in vitro. *J Immunol* 175:3475–3483. <https://doi.org/10.4049/jimmunol.175.6.3475>
114. Kluger MA, Zahner G, Paust H-J et al (2013) Leukocyte-derived MMP9 is crucial for the recruitment of proinflammatory macrophages in experimental glomerulonephritis. *Kidney Int* 83:865–877. <https://doi.org/10.1038/ki.2012.483>

**Publisher's Note** Springer Nature remains neutral with regard to jurisdictional claims in published maps and institutional affiliations.

Springer Nature or its licensor (e.g. a society or other partner) holds exclusive rights to this article under a publishing agreement with the author(s) or other rightsholder(s); author self-archiving of the accepted manuscript version of this article is solely governed by the terms of such publishing agreement and applicable law.